Ar-Matrix IR Spectra of 5-Halouracils Interpreted by Means of DFT Calculations

ARTICLE *in* THE JOURNAL OF PHYSICAL CHEMISTRY A · APRIL 2005

Impact Factor: 2.69 · DOI: 10.1021/jp045213f · Source: PubMed

6 AUTHORS, INCLUDING:

Joanna E Rode
Instytut Chemii Przemysłowej
38 PUBLICATIONS **516** CITATIONS
SEE PROFILE

Michał Henryk Jamróz
Institute of Nuclear Chemistry and Technolo…
70 PUBLICATIONS **877** CITATIONS
SEE PROFILE

Krzysztof Bajdor
Institute of Industrial Organic Chemistry
49 PUBLICATIONS **663** CITATIONS
SEE PROFILE

Ar-Matrix IR Spectra of 5-Halouracils Interpreted by Means of DFT Calculations

Jan Cz. Dobrowolski,*,†,‡ Joanna E. Rode,† Robert Kołos,§ Michał H. Jamróz,† Krzysztof Bajdor,† and Aleksander P. Mazurek‡

Industrial Chemistry Research Institute, Rydygiera 8, 01-793 Warsaw, Poland, National Institute of Public Health, Chełmska 30/34, 00-725 Warsaw, Poland, and Institute of Physical Chemistry, Polish Academy of Sciences, Kasprzaka 44, 01-224 Warsaw, Poland

Received: October 20, 2004; In Final Form: January 11, 2005

The infrared low-temperature Ar-matrix spectra of 5-halouracils and unsubstituted uracil were measured and interpreted in terms of the spectra calculated at the DFT/B3PW91/6-311G** level followed by a potential energy distribution (PED) analysis. For the PED analysis, the sets of halouracil mode definitions were constructed so that dissimilarities in the interpretations of the different spectra were minimized. Anharmonic frequency calculations enabled more light to be shed on the Fermi resonance (FR) phenomena occurring in the ν(C═O) stretching vibrations region. For each halouracil vibrational spectrum, several FRs manifest themselves in the ν(C═O) stretching vibrations region. We show that the most frequent components participating in these resonances are the $\nu(C_4{=}O_{10})$ frequency, a β(N−H) mode frequency, and a β(C═O) mode frequency. The experimental ν(N−H) frequencies are reproduced by the calculated anharmonic frequencies better than by the scaled harmonic ones, and the ν(C═O) frequencies respond in the opposite manner. The experimental frequencies located below 1500 cm^{-1} are reproduced equally well by the two kinds of calculations.

Introduction

Since it was found that certain tumors incorporate uracil into DNA in preference to thymine, 5-fluorouracil (FU; first introduced into medicine in 1957) has been widely used in the treatment of cancer (cf. refs 1−4). FU itself also exhibits antibacterial activity[5] and augments the bactericidal effect of antibiotics.[6] The other 5-halouracils have exhibited weaker antiviral and antibacterial activity than FU.[7] However, some 5-iodouracil (IU) based nucleoside analogues were found to be selective inhibitors of herpes simplex viruses,[8,9] and the others (developed to treat hepatic B infections) were shown to be toxic when incorporated into mitochondrial DNA.[10]

The biology and chemistry of the halogenated uracils have been explored as possible means of sensitizing DNA to ionizing radiation.[11−14] Their electron affinities, greater than those of other nucleic acid bases, make halouracils capture electrons and dehalogenate; however, their radiosensitization properties are less effective in double-stranded DNA than in single-stranded DNA.[14] So far, radiosensitization of halouracils has not been utilized clinically.[15] Chlorinated pyrimidines [5-chlorouracil (ClU) included] are effective mutagens, clastogens, and toxicants as well as extremely effective inducers of sister-chromatid exchanges.[15]

The 5-halouracils substitute thymine in a single- or double-stranded DNA (cf. refs 14 and 16−18), and they also act by substituting uracil in RNA [e.g., FU and 5-bromouracil (BrU)[19]]; for example, they change the interactions of nucleic acids with proteins by inducing various biological phenomena.[16] 5-Halouracils have also served as repair-system models to study damaged DNA.[17] BrU−guanine base pairs have been shown to act as intermediates in 5-bromodeoxyuridine-induced transition mutation pathways.[18] Again, with increasing pH, the efficiency of FU or BrU to form correct base pairs with adenine has been found to decrease 4- and 8-fold; ionized 5-halouracils can form mispairs with guanine.[20] Quite recently, it has been suggested that peroxidases secreted by human phagocytes facilitate the formation of ClU and BrU (which are well-known mutagens) in the human inflammatory tissue.[21,22] Halouracils can form metal ternary complexes Me(HU)(HISD), where HU stands for halouracil; Me is a divalent Mn, Co, Ni, Cu, Zn, or Cd cation; and HISD is histidine, which exhibits an antitumor activity too.[23] There are also well-known metal complexes with adenine as the primary ligand and halouracil as the secondary ligand.[24] The X-ray structures of uracil and 5-halouracils were solved up to the mid-1970s.[25−28]

Considering the importance of 5-halouracils for medicinal chemistry, it is surprising that their vibrational spectra, taken for low-temperature matrixes and for the polycrystalline state, have been looked into relatively little and that the literature assignments of a number of fundamental vibrations are often in conflict.[29−52]

Recently, we have investigated some selected stretching modes in 5-halouracil vibrational spectra for both the Ar-matrix and the solid state;[51,52] theoretical and experimental ^{1}H, ^{13}C, ^{15}N, and ^{17}O NMR spectra;[53] mass electron- and chemical-ionization spectra; and negative and positive ion atmospheric-pressure chemical-ionization spectra.[54] We have also studied theoretical and experimental NMR spectra of 5-nitro-, 5-amino-, and 5-carboxyuracils[55] and vibrational spectra of 5-carboxyuracil and its alkali-metal salts.[56]

The aim of this study is to make a reliable assignment of the vibrational modes in the Fourier-transform infrared (FTIR)

* Author to whom correspondence should be addressed. E-mail: janek@il.waw.pl, Jan.Dobrowolski@ichp.pl.
† Industrial Chemistry Research Institute.
‡ National Institute of Public Health.
§ Polish Academy of Sciences.

10.1021/jp045213f CCC: $30.25
Published on Web 02/18/2005

spectra of 5-halouracils trapped in low-temperature Ar matrixes. In addition to our paper, which describes only general trends in the ν(N−H) and ν(C═O) stretching vibrations regions of the Ar-matrix low-temperature IR spectra of 5-halouracils,[51] such spectra have been taken for FU[29,38] and BrU[38,39] only. However, just for BrU, the interpretation was supported by MINDO/3 calculations. On the other hand, the ample literature data devoted to the vibrational spectra of uracil[29−38] are helpful for the assignment of the 5-halouracils' vibrational spectra only partially: two C−H oscillators present in the uracil molecule result in CH and NH bending-mode couplings and make the spectral picture knotty.

In this paper, the DFT/B3PW91/6-311G**-calculated spectra were interpreted in terms of the potential energy distribution (PED) on the basis of local mode definitions unified for all 5-halouracils. Moreover, the local modes of uracil, serving as a kind of reference molecule, were described by using definitions as close to those used for 5-halouracils as possible. This approach allows one to describe the IR spectra of 5-halouracils consistently.

Experimental Section

Sigma's 99 wt % uracil and 5-halouracils were used. The Ar matrixes were prepared within a Displex (Air Products) closed-cycle helium refrigerator. Ar gas (Aldrich, 99.998%) was passed over crystalline uracil, and 5-halouracils were placed in a heated tube (370−450 K), before being solidified at 19 K on the surface of the CsI window, transparent to the IR radiation in the spectral range of interest. The typical Ar flow rate was 10^{-3} mol/h. The molar ratio of Ar to the molecules under study was not known. However, care was taken to avoid the aggregation of deposited molecules; the vaporization temperature was always set to the lowest possible value that still led to quantifiable IR absorption signals. Spectra were measured by using a Nicolet 170SX FTIR spectrometer (HgCdTe detector, KBr beam splitter, range 450−4000 cm^{-1}, resolution 1 cm^{-1}).

Calculations

The density-functional-theory (DFT) quantum-chemical calculations were performed by using the *Gaussian 03* packages of programs[57] run on the Cray SV1-1A supercomputer at the Interdisciplinary Center of Mathematical and Computer Modeling at Warsaw University. The halouracil structures were optimized, and the analytical harmonic and anharmonic frequencies as well as the IR intensities and Raman activities were calculated at the DFT/B3PW91/6-311G** level. Using a moderately large basis set allowed us to perform time- and memory-consuming anharmonic calculations essential for the explanation of the Fermi resonance (FR) range of the experimental spectra. The anharmonic vibrations calculation code implemented in *Gaussian 03* is based on the second-order perturbative treatment of anharmonic effects by the use of effective, finite-difference evaluations of third and semidiagonal fourth derivatives.[58,59] On the other hand, until very recently,[60] the B3PW91 exchange correlation functional, quite similar to the B3LYP functional,[61] has been shown to yield fairly good frequencies.[63,65] No imaginary frequency was present in the DFT-calculated spectra. The PED calculations were carried out with the aid of the VEDA program.[64] The calculated harmonic frequencies were next scaled by following the Palafox method,[62] which, for the B3PW91/6-311G** computations, results in the following scaling straight line: $\nu_{scal} = 0.954\nu_{calc} + 27.6$.

CHART 1 Structure and Atom Numbering of 5-Halouracils (X = H, F, Cl, Br, and I)

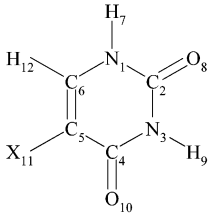

Results and Discussion

Uracil and halouracil molecules are planar, six-membered-ring heterocycle molecules built from 12 atoms (Chart 1). Thus, each of the molecules exhibits 30 fundamental vibrations, 21 of which are in-plane and 9 of which are out-of-plane; that is, they belong to either the A′ or A″ representation of the C_s group of point symmetry, respectively. The matrix IR spectra of 5-halouracils are more complex than the above description would suggest: the FR phenomenon, occurring in the carbonyl stretching vibrations region, makes the spectra much more complicated. The presence of the two conjugated amide NHCO groups fixed in a cis configuration would enable a discussion about some vibrational modes in terms of amide bands, where the amide I band corresponds to the C═O stretching band, the amide II band represents the in-plane N−H bending vibrations band, the amide III band denotes the C−N stretching, the amide IV band indicates the in-plane C═O bending band, and so forth. However, in the case of the 5-halouracils spectra, the amide bands are doubled, and here we do not use that notation because it is less informative than the notation resulting from the PED analysis.

The experimental Ar-matrix IR spectra of 5-halouracils were interpreted by basing them on calculated (scaled[62]) harmonic and anharmonic frequencies, followed by the PED analysis. The PED analysis was grounded in the uniform set of mode definitions (Table 1S, the Supporting Information), enabling the theoretical spectra to be consistently examined. Table 1S also contains analogous definitions for the uracil modes that are different from those of 5-halouracils. The experimental and calculated frequencies as well as the calculated IR intensities, Raman activities, and depolarization ratios for uracil, FU, ClU, BrU, and IU are gathered in Tables 1−5, respectively. The list of modes predicted to participate with the ν(C═O) modes in FRs is presented in Table 6. Table 2S in the Supporting Information juxtaposes the experimental frequencies of all of the molecules studied. The experimental spectra supported by the calculated ones are presented in Figures 1−5.

ν(N−H) Stretching Vibrations. *DFT Calculations.* The calculations predicted the two stretching N−H bands to occur within the range 3450−3500 cm^{-1} and the N−H oscillators to be uncoupled (Tables 1−5). The $\nu(N_1-H_7)$ band is estimated to occur at wavelengths ca. 40 cm^{-1} higher than those of the $\nu(N_3-H_9)$ band. According to the harmonic frequency calculations, as the halogen mass is increased, the two bands shift slightly toward lower wavenumbers and the ν(N−H) band separation is likely to decrease: 43.5, 40.3, 39.2, and 37.6 cm^{-1}, for FU, ClU, BrU, and IU, respectively. The anharmonic frequency calculations predict neither monotonic frequency shifts nor anharmonicity changes of the ν(N−H) bands to occur with an increase in the halogen mass (Tables 1−5). For unsubstituted uracil,[65] the bands are located similarly to those of the FU molecule. The intensity of the $\nu(N_1-H_7)$ band is calculated to be ca. 1.5 times higher than that of the $\nu(N_3-H_9)$ band.

TABLE 1: Bands Observed (ν_{exp}, cm^{-1}) in the Ar-Matrix IR Spectrum of Uracil Compared with the B3PW91/6-311G-Calculated Wavenumbers (ν_{anh}, ν_{scal}, cm^{-1}) Interpreted in Terms of the PEDs (in Percentages Not Lower than 10%)[a]**

	sym	ν_{exp}[b]	ν_{anh}	ν_{scal}	I_{IR}	R_A	ρ	% PED	ref 30
					In-Plane Modes				
1	A′	3483.5	3496.8	3520.0	106.6	90.8	0.245	$100\nu(N_1-H_7)$	3484
2	A′	3434.0	3452.9	3480.5	67.0	73.4	0.282	$100\nu(N_3-H_9)$	3434
3	A′	nd	3120.0	3133.1	1.0	100.0	0.231	$96\nu(C_5-H_{11})$	3094
4	A′	nd	3110.5	3091.7	3.5	94.7	0.404	$96\nu(C_6-H_{12})$	3079
5	A′	1774.0 FR, 1770.0 FR, 1763.5 FR, 1761.0 FR, 1757.0 FR	1811.7	1789.5	620.0	10.8	0.167	$73\nu(C_2=O_8)$	1763
6	A′	1733.0 FR, 1730.5 FR, 1728.0 FR, 1706.0 FR, 1703.5 FR, 1698.5 FR	1785.2	1751.2	632.2	38.0	0.280	$77\nu(C_4=O_{10})$	1728
7	A′	nd	1653.0	1638.8	71.0	19.3	0.104	$71\nu(C_5=C_6)$	1643
8	A′	1471.5	1468.5	1470.7	105.1	9.6	0.593	$39\beta(N_1-H_7)+17\nu_2(R)-13\nu(C_2=O_8)$	1471
9	A′	1399.5	1385.9	1384.6	41.4	0.3	0.629	$31\nu_3(M)-25\beta(N_3-H_9)+20\beta(C_6-H_{12})$	1388
10	A′	1388.5	1378.3	1376.2	75.9	0.9	0.388	$43\beta(N_3-H_9)+12\nu_3(M)-12\beta(N_1-H_7)$	1380
11	A′	1380.5	1354.0	1350.9	28.3	13.1	0.403	$54\beta(C_6-H_{12})+11\nu_2(R)$	1399
12	A′	1217.5	1197.3	1200.9	3.7	12.4	0.484	$44\beta(C_5-H_{11})+25\nu^{as}(CN)+11\nu_1(R)$	1217
13	A′	1184.0	1172.1	1174.3	95.1	1.4	0.245	$47\nu_2(R)-18\beta(C_5-H_{11})$	1184
14	A′	1075.5, 1068.5	1068.9	1069.9	7.1	6.7	0.332	$34\nu^{as}(CN)-19\beta(C_5-H_{11})+12\beta(N_1-H_7)$	1075
15	A′	982.5 ?	983.9	975.9	6.2	0.2	0.087	$59\beta_1(R)-20\nu(B)$	981
16	A′	958.5	950.1	955.3	6.5	2.7	0.440	$36\nu_1(R)+14\beta(N_3-H_9)-11\nu^{as}(CN)$	958
17	A′	nd	756.2	767.9	2.3	19.7	0.092	$67\nu(B)+12\beta_1(R)$	767
18	A′	nd	550.9	563.7	3.6	2.5	0.651	$74\beta^{s}(C=O)$	556
19	A′	536.5	535.3	546.3	6.9	4.8	0.368	$75\beta_3(R)$	536
20	A′	516.5	514.0	524.3	18.8	2.0	0.705	$84\beta_2(R)$	516
21	A′	or	388.8	399.0	21.3	1.8	0.699	$69\beta^{as}(C=O)-15\nu_3(M)$	394
					Out-of-Plane Modes				
22	A″	nd	950.7	955.5	0.5	1.6	0.736	$73\gamma(C_6-H_{12})$	944
23	A″	804.0	812.2	811.8	74.4	0.7	0.750	$70\gamma(C_5-H_{11})$	804
24	A″	756.5	767.4	770.4	40.8	0.0	0.750	$84\gamma(C_2=O_8)$	756
25	A″	718.0	724.4	728.6	15.0	1.6	0.750	$56\gamma(C_4=O_{10})+12\gamma(C_5-H_{11})-11\gamma_1(R)-10\gamma(C_2=O_8)$	719
26	A″	662.0	667.8	688.5	72.3	2.0	0.750	$86\gamma(N_3-H_9)$	662
27	A″	551.0	570.2	575.7	45.2	0.8	0.750	$87\gamma(N_1-H_7)$	551
28	A″	or	393.9	407.5	25.3	1.6	0.750	$63\gamma_1(R)+22\gamma(C_4=O_{10})$	401
29	A″	or	166.2	188.1	0.1	0.8	0.750	$75\gamma_3(R)-10\gamma_1(R)$	
30	A″	or	150.6	172.0	1.2	0.0	0.750	$76\gamma_2(R)+16\gamma_3(R)$	

[a] Calculated frequencies are scaled[62] by the straight line $\nu_{scal} = 0.954\nu_{calc} + 27.6$; I_{IR} stands for IR intensities (km mol^{-1}), R_A denotes Raman activities (Å amu^{-1}), and ρ stands for the depolarization ratio. For local mode definitions, see Table 1S in the Supporting Information. [b] FR denotes involvement of the band in a Fermi resonance, nd stands for not determined, or stands for out of range, and ? is used when the assignment is questionable.

Ar-Matrix IR Spectra. The measurements show that, in the case of high-frequency fundamentals, the scaled DFT frequencies overestimate the positions of the experimental bands by ca. 40 cm^{-1} (Tables 1−5). Nevertheless, the presence of only two bands between 3400 and 3500 cm^{-1} (Figure 1) allows the assignment of the two ν(N−H) bands beyond any doubt. As the halogen mass is increased (Table 2S in the Supporting Information), they shift slightly toward lower frequencies and the band separation changes as follows: 52.5, 46.0, 45.0, 44.0 cm^{-1} for FU, ClU, BrU, and IU, respectively. For unsubstituted uracil, it is equal to 49.5 cm^{-1}. Similar tendencies were observed by us in an earlier study.[51]

$\nu(C_6-H_{12})$ and $\nu(C_5-X_{11})$ Stretching Vibrations. Except for that of the uracil molecule, in which there are two C−H oscillators, the $\nu(C_6-H_{12})$ band could be observed for halouracils, provided it had a sufficiently high intensity (Tables 1−5). The experimental data for uracil[30] (Table 1) and BrU[38] (Table 4) allow us to see that both anharmonic and scaled harmonic frequency calculations are likely to overestimate the positions of both the $\nu(C_5-H_{11})$ and $\nu(C_6-H_{12})$ bands by ca. 10−50 cm^{-1}. The calculations predict that, as the substituent mass at position C5 is increased, the $\nu(C_6-H_{12})$ band shifts toward lower wavenumbers and its intensity decreases (Tables 1−5). The anharmonic frequency calculations reveal no monotonic frequency shifts of the $\nu(C_6-H_{12})$ bands occurring with an increase in the halogen mass (Tables 1−5). The weak intensity of the $\nu(C_6-H_{12})$ band made it absent in the experimental spectra recorded.

The $\nu(C_5-F_{11})$ local mode is predicted to contribute substantially to the vibration at 1250 cm^{-1}, which agrees perfectly well with the experimental band frequency and the literature data[53] (Table 2). According to PED analysis, the $\nu(C_5-Cl_{11})$ local mode is spread out between three normal modes that absorb at ca. 1070, 655 (the largest PED = 31%), and 370 cm^{-1} (Table 3). A similar situation occurs for the $\nu(C_5-Br_{11})$ local mode, which is spread out between the normal modes predicted to absorb at 1047, 623, and ca. 290 cm^{-1} (the largest PED = 46%) (Table 4). In the case of the IU molecule, the local $\nu(C_5-I_{11})$ mode contributes mainly to the vibration at 258 (harmonic) or 240 cm^{-1} (anharmonic) (Table 5). The

TABLE 2: Bands Observed (ν_{exp}, cm^{-1}) in the Ar-Matrix IR Spectrum of FU Compared with the B3PW91/6-311G-Calculated Wavenumbers (ν_{anh}, ν_{scal}, cm^{-1}) Interpreted in Terms of the PEDs (in Percentages Not Lower than 10%)[a]**

	sym	ν_{exp}[b]	ν_{anh}	ν_{scal}	I_{IR}	R_A	ρ	% PED	refs
					In-Plane Modes				
1	A′	3480.0	3498.3	3523.5	116.8	88.7	0.246	$100\nu(N_1-H_7)$	3468[29,38]
2	A′	3427.5	3450.2	3479.0	75.4	68.6	0.285	$100\nu(N_3-H_9)$	3416[29,38]
3	A′	nd	3100.4	3110.0	2.8	102.3	0.322	$99\nu(C_6-H_{12})$	
4	A′	1780.0 FR, 1778.0 FR, 1768.0 FR, 1761.0 FR, 1755.0 FR	1813.1	1791.5	581.1	11.4	0.169	$73\nu(C_2=O_8)$	1781−1706,[29] 1742[38]
5	A′	1746.5 FR, 1742.5 FR, 1708.5 FR, 1705.5 FR	1785.5	1759.9	632.3	42.0	0.262	$78\nu(C_4=O_{10})$	1781−1706,[29] 1754,[38] 1781−1706[29]
6	A′	1686.5, 1684.5	1695.9	1679.6	36.7	33.9	0.100	$71\nu(C_5=C_6)$	1621,[29] 1685[38]
7	A′	1472.0	1471.7	1471.6	47.5	6.9	0.610	$31\beta(N_1-H_7) - 19\nu_3(M) + 13\nu_2(R)$	1477[29,38]
8	A′	1400.5	1397.6	1397.5	64.3	3.4	0.740	$29\nu_3(M) + 21\beta(N_1-H_7) - 11\beta^{as}(C=O)$	1412[38]
9	A′	1367.0	1370.5	1373.2	13.3	1.7	0.741	$64\beta(N_3-H_9)$	1399,[29] 1386[38]
10	A′	1333.5	1323.9	1316.8	17.7	27.5	0.394	$46\beta(C_6-H_{12}) + 16\nu_2(R) + 11\nu_1(R)$	1182,[38] 1334[c,38]
11	A′	1247.5	1248.9	1249.5	247.0	4.4	0.196	$44\nu(C_5-F_{11}) + 14\nu_3(M) + 14\beta_1(R)$	1253,[29] 1247[c,38]
12	A′	1184.0, 1180.7	1159.6	1165.2	79.1	2.7	0.395	$41\nu_2(R) - 21\beta(C_6-H_{12}) + 11\nu^{as}(CN)$	
13	A′	1147.0, 1145.5sh	1135.8	1139.3	24.3	1.7	0.724	$45\nu^{as}(CN) + 18\beta(N_1-H_7)$	
14	A′	959.5	957.4	958.4	12.6	1.8	0.333	$48\nu_1(R)$	1050[38]
15	A′	806.5	806.0	810.1	33.1	4.6	0.134	$57\beta_1(R) - 16\nu(C_5-F_{11})$	876,[38] 807[d,38]
16	A′	nd	728.5	740.6	10.5	14.1	0.080	$68\nu(B)$	731[38]
17	A′	nd	627.1	632.0	2.1	5.9	0.610	$69\beta^{s}(C=O)$	539[29,38]
18	A′	532.0	530.3	540.4	6.4	4.8	0.423	$61\beta_3(R)$	
19	A′	451.0	449.7	463.0	7.2	3.1	0.581	$76\beta_2(R)$	
20	A′	or	390.3	402.0	18.8	1.5	0.629	$60\beta^{as}(C=O) + 12\nu_3(M) - 11\nu^{as}(CN)$	393[29]
21	A′	or	300.4	315.7	1.0	0.4	0.498	$81\beta(C_5-F_{11})$	
					Out-of-Plane Modes				
22	A″	876.5	882.1	876.8	33.6	2.9	0.750	$93\gamma(C_6-H_{12})$	961[38]
23	A″	757.5	766.3	770.3	56.3	1.4	0.750	$66\gamma(C_4=O_{10}) + 10\gamma_1(R) - 10\gamma(C_2=O_8)$	806,[29] 757[38]
24	A″	749.5	757.7	760.7	22.6	0.6	0.750	$83\gamma(C_2=O_8) - 13\gamma(C_4=O_{10})$	757,[29] 750[38]
25	A″	653.0	663.4	679.0	59.5	2.1	0.750	$86\gamma(N_3-H_9)$	653[29,38]
26	A″	527.0	537.2	556.4	63.1	0.8	0.750	$94\gamma(N_1-H_7)$	571[29,38]
27	A″	or	379.6	393.0	11.3	1.9	0.750	$68\gamma_1(R) + 15\gamma(C_4=O_{10})$	
28	A″	or	352.8	363.5	7.6	0.3	0.750	$87\gamma(C_5-F_{11})$	
29	A″	or	153.2	174.3	0.9	0.1	0.750	$90\gamma_2(R)$	
30	A″	or	116.4	139.6	1.5	0.4	0.750	$81\gamma_3(R)$	

[a] Calculated frequencies are scaled[62] by the straight line $\nu_{scal} = 0.954\nu_{calc} + 27.6$; I_{IR} stands for IR intensities (km mol^{-1}), R_A denotes Raman activities (Å amu^{-1}), and ρ stands for the depolarization ratio. For local mode definitions, see Table 1S in the Supporting Information. [b] FR denotes involvement of the band in a Fermi resonance, nd stands for not determined, and or stands for out of range. [c] In ref 38, the band is assigned to a ring-stretching mode. [d] In ref 38, the band is assigned to the C−F-stretching mode.

$\nu(C_5-X_{11})$ mode is the only vibration of decreasing anharmonicity induced by going from a FU to an IU molecule (Tables 1−5).

ν(C=O) Stretching Vibrations. *DFT Calculations.* The scaled harmonic frequency calculations predict the $\nu(C_2=O_8)$ band to occur at ca. 1790 cm^{-1} and the $\nu(C_4=O_{10})$ band at ca. 40 cm^{-1} below that (Figure 2; Tables 1−5). Unexpectedly, the anharmonic frequency calculations predict the two modes to occur at wavenumbers higher, by ca. 25 cm^{-1}, than those of the corresponding scaled harmonic frequencies. This may suggest that, in the carbonyl stretching vibrations region, the anharmonic frequencies describe the experimental bands less accurately than do the scaled harmonic values. The two ν(C=O) modes do not have PEDs smaller than 70%; thus, they are not coupled (Tables 1−5). Regardless of the C5 substitution, the $\nu(C_2=O_8)$ band's position is predicted to remain almost unaffected by changes in the molecular structure (1790 cm^{-1} harmonic, 1813 cm^{-1} anharmonic; Tables 1−5). This is caused by the fact that the $C_2=O_8$ moiety is quite distanced from the C_5-X_{11} group and, moreover, it is surrounded by the two N−H groups, which buffer it from influences of the remaining molecular moieties (Chart 1). On the other hand, the $C_4=O_{10}$ moiety neighbors the C_5-X_{11} group, and as the halogen mass is increased, the corresponding $\nu(C_4=O_{10})$ harmonic mode drifts slightly toward lower wavenumbers (from ca. 1760 cm^{-1} for FU to ca. 1750 cm^{-1} for IU; Tables 1−5). However, the anharmonic approximation suggests that only for the IU molecule is the position of the $\nu(C_4=O_{10})$ mode significantly shifted toward lower frequencies. The two band intensities are practically equal for uracil and FU. For heavier halogens, the $\nu(C_2=O_8)$ band intensity increases, whereas the $\nu(C_4=O_{10})$ band intensity decreases proportionally so that, for the IU molecule, the former is twice as intense as the latter (Tables 1−5).

Ar-Matrix IR Spectra. The experimental spectra of halouracils in the C=O stretching vibrations region are quite complex, yet the most complicated spectrum is that of uracil itself (Figure 2). For halouracils and uracil, one can distinguish three groups of bands: the first located at ca. 1765 cm^{-1}, the second in the region of 1720−1745 cm^{-1}, and the third between 1705 and 1710 cm^{-1} (Figure 2). The positions of the first and third (groups

TABLE 3: Bands Observed (ν_{exp}, cm^{-1}) in the Ar-Matrix IR Spectrum of ClU Compared with the B3PW91/6-311G-Calculated Wavenumbers (ν_{anh}, ν_{scal}, cm^{-1}) Interpreted in Terms of the PEDs (in Percentages Not Lower than 10%)[a]**

	sym	ν_{exp}[b]	ν_{anh}	ν_{scal}	I_{IR}	R_A	ρ	% PED
				In-Plane Modes				
1	A′	3472.0	3481.1	3517.8	122.3	103.7	0.235	$100\nu(N_1-H_7)$
2	A′	3426.0	3455.2	3477.5	78.1	81.3	0.282	$100\nu(N_3-H_9)$
3	A′	nd	3088.0	3106.4	1.5	80.8	0.342	$99\nu(C_6-H_{12})$
4	A′	1768.5 FR, 1764.0 FR	1811.5	1792.9	708.4	15.1	0.192	$74\nu(C_2=O_8)$
5	A′	1735.5 FR, 1729.0 FR, 1709.5 FR	1783.2	1759.0	516.9	31.3	0.305	$82\nu(C_4=O_{10})$
6	A′	1640.5	1646.9	1637.5	65.7	48.1	0.142	$69\nu(C_5=C_6) - 11\beta(C_6-H_{12})$
7	A′	1460.5	1460.0	1463.1	77.2	11.4	0.567	$42\beta(N_1-H_7) + 14\nu_2(R) - 13\nu_3(M) - 10\nu(C_2=O_8)$
8	A′	1392.5	1383.4	1382.3	66.0	2.1	0.750	$35\nu_3(M) + 26\beta(N_3-H_9)$
9	A′	1387.0	1370.7	1370.8	45.4	1.1	0.736	$47\beta(N_3-H_9) - 17\beta(N_1-H_7) - 19\nu_3(M) + 11\beta^{as}(C=O)$
10	A′	1333.0	1315.2	1312.8	8.2	22.7	0.330	$52\beta(C_6-H_{12}) + 13\nu(C_5=C_6) + 13\nu_2(R)$
11	A′	1186.0, 1184.5sh	1169.8	1172.9	92.4	1.9	0.505	$46\nu_2(R) - 20\beta(C_6-H_{12}) - 11\beta(N_1-H_7)$
12	A′	1160.5	1150.8	1158.6	34.4	2.0	0.734	$58\nu^{as}(CN) - 10\beta(N_1-H_7)$
13	A′	1073.0	1071.1	1066.3	72.3	0.3	0.742	$46\beta_1(R) - 23\nu(C_5-Cl_{11}) + 12\nu(B)$
14	A′	964.0	961.3	960.7	13.6	2.6	0.602	$53\nu_1(R)$
15	A′	nd	782.6	775.6	6.8	18.7	0.090	$49\nu(B) - 29\beta_1(R)$
16	A′	652.5	656.9	664.7	44.0	1.8	0.126	$37\beta_2(R) - 31\nu(C_5-Cl_{11}) - 14\nu(B)$
17	A′	nd	604.1	610.2	0.1	6.2	0.448	$73\beta^{s}(C=O)$
18	A′	533.0	532.0	542.3	7.8	4.1	0.346	$66\beta_3(R)$
19	A′	or	405.0	416.6	16.5	4.1	0.521	$52\beta^{as}(C=O) + 14\nu_3(M) + 10\nu^{as}(CN)$
20	A′	or	361.7	375.2	6.7	2.1	0.430	$38\beta_2(R) + 21\nu(C_5-Cl_{11}) + 10\beta^{as}(C=O)$
21	A′	or	226.9	244.9	0.4	1.3	0.733	$81\beta(C_5-Cl_{11})$
				Out-of-Plane Modes				
22	A″	895.5	894.0	899.5	16.3	1.6	0.750	$93\gamma(C_6-H_{12})$
23	A″	758.0	774.4	778.7	60.5	0.5	0.750	$69\gamma(C_4=O_{10}) - 11\gamma_1(R)$
24	A″	750.5	759.5	761.3	25.0	0.2	0.750	$88\gamma(C_2=O_8)$
25	A″	656.5	660.1	677.9	63.1	2.3	0.750	$86\gamma(N_3-H_9)$
26	A″	545.5	547.9	570.0	60.0	0.7	0.750	$92\gamma(N_1-H_7)$
27	A″	or	385.1	400.1	23.4	1.4	0.750	$70\gamma_1(R) + 13\gamma(C_4=O_{10})$
28	A″	or	293.3	308.8	0.0	0.1	0.750	$88\gamma(C_5-Cl_{11})$
29	A″	or	151.2	172.9	1.1	0.1	0.750	$88\gamma_2(R)$
30	A″	or	96.9	121.1	1.3	0.3	0.750	$82\gamma_3(R)$

[a] Calculated frequencies are scaled[62] by the straight line $\nu_{scal} = 0.954\nu_{calc} + 27.6$; I_{IR} stands for IR intensities (km mol^{-1}), R_A denotes Raman activities (Å amu^{-1}), and ρ stands for the depolarization ratio. For local mode definitions, see Table 1S in the Supporting Information. [b] FR denotes involvement of the band in a Fermi resonance, nd stands for not determined, and or stands for out of range.

of) C═O stretching vibrations bands are almost insensitive to the change in the mass of the substituent, whereas the middle band shifts from ca. 1740 to 1720 cm^{-1} on passing from the FU to the IU molecule. For the uracil molecule, the middle group of bands is positioned at a wavenumber similar to that for BrU, that is, at ca. 1728 cm^{-1}. Within each group of bands, the bands are split, probably because of the formation of diverse Ar clusters surrounding the molecules in the matrixes. Thus, let us assume that the spectral pattern can be explained in terms of three vibrations; however, the calculations predicted only two bands in this region. The most probable effect responsible for the increase in the number of groups of ν(C═O) bands is a FR. Although we observe minute amounts of water and carbon dioxide in the matrixes measured, we exclude the possibility of any intermolecular interaction accounting for the appearance of a new band. Out of three of the publications on IR spectra of halouracils in cryogenic matrixes,[29,38,39] only Nowak[29] explained the knotty pattern of the ν(C═O) region in terms of a FR; the origin of the resonance remained unresolved, however.

Fermi Resonance. Let us now consider the various hypotheses that try to explain the origin of the FR in the C═O stretching vibrations region. First, notice that, on the basis of harmonic frequencies, it is difficult to decide which of the C═O bands participates in the resonance. As the halogen mass is increased, the middle experimental band shifts toward lower wavenumbers; however, this may suggest that either the band at ca. 1765 cm^{-1} is in the resonance and the resonance splitting increases as the halogen mass is increased or the band at ca. 1705 cm^{-1} is in the resonance and the resonance splitting decreases as the halogen mass is increased. Second, the FR does not have to be of the same origin for all of the molecules studied, yet such an interpretation is desirable. The fact that the two ν(C═O) bands belong to the A′ representation of the C_s symmetry group introduces, however, a limitation for the resonating overtones or combinational tones: the only modes that may resonate with the ν(C═O) modes are those that belong to the A′ representation; that is, they must belong either to the A′⊗A′ or to the A″⊗A″ direct product. Except for the $\gamma(C_6-H_{12})$ mode, all of the other A″ symmetry overtone modes absorb at frequencies too low to resonate with the ν(C═O) bands (Table 6). However, for uracil, the $\gamma(C_6-H_{12})$ mode overtone would absorb at frequencies just slightly too high to resonate, that is, at ca. 1850 cm^{-1}. Now, note that none of the A′ symmetry bands has an overtone in the proper wavenumber range (Table 6). Thus, a combination of two A′ symmetry tones is responsible for the FR in the C═O stretching vibrations region. It was shown for uracil that deuteration at the two uracil N atoms clarifies the pattern in the C═O stretching vibrations region so that two main bands appear.[30,32,37] Moreover, from among the IR matrix spectra of N_1-, N_3-, and C_5-methylated uracils and those of N_1- and N_3-dimethylated uracils, only those that are methylated at the N_3 position exhibit two main bands in the ν(C═O) stretching

TABLE 4: Bands Observed (ν_{exp}, cm^{-1}) in the Ar-Matrix IR Spectrum of BrU Compared with the B3PW91/6-311G-Calculated Wavenumbers (ν_{anh}, ν_{scal}, cm^{-1}) Interpreted in Terms of the PEDs (in Percentage Not Lower than 10%)[a]**

	sym	ν_{exp}[b]	ν_{anh}	ν_{scal}	I_{IR}	R_A	ρ	% PED	refs
					In-Plane Modes				
1	A′	3470.5	3490.1	3516.2	123.7	110.2	0.235	$100\nu(N_1-H_7)$	3459,[38] 3471[39]
2	A′	3424.5	3455.6	3477.0	78.5	87.8	0.286	$100\nu(N_3-H_9)$	3413,[38] 3425[39]
3	A′	nd	3092.7	3105.0	0.9	72.6	0.346	$99\nu(C_6-H_{12})$	3040[38]
4	A′	1766.5 FR, 1762.5 FR	1814.2	1792.5	752.2	16.6	0.207	$74\nu(C_2=O_8)$	1761,[38] 1763[39]
5	A′	1729.0 FR, 1711.5 FR, 1704.5 FR	1784.9	1755.3	472.3	28.5	0.326	$83\nu(C_4=O_{10})$	1729[38,39]
6	A′	1634.5	1638.2	1629.2	75.9	48.8	0.158	$68\nu(C_5=C_6) - 12\beta(C_6-H_{12})$	1635,[38] 1711[39]
7	A′	1459.0	1460.6	1460.2	79.5	11.4	0.566	$44\beta(N_1-H_7) + 14\nu_2(R) - 11\nu_3(M) - 11\nu(C_2=O_8)$	1463,[38] 1377[39]
8	A′	1390.5	1377.0	1379.9	61.9	2.5	0.730	$31\nu_3(M) + 34\beta(N_3-H_9)$	1400,[38,c] 1390[39]
9	A′	1378.0	1370.9	1369.5	64.2	0.7	0.750	$38\beta(N_3-H_9) - 19\beta(N_1-H_7) - 19\nu_3(M) + 13\beta^{as}(C=O)$	1397,[38] 1327 [39]
10	A′	1328.5	1317.6	1313.0	9.8	21.8	0.321	$53\beta(C_6-H_{12}) + 14\nu(C_5=C_6) + 13\nu_2(R)$	1192,[38] 1189,[39] 1327[c,38]
11	A′	1190.0, 1187.0sh	1174.3	1172.8	90.0	1.7	0.582	$47\nu_2(R) - 19\beta(C_6-H_{12}) - 12\beta(N_1-H_7)$	
12	A′	1155.5, 1153.0	1144.3	1150.2	22.3	2.1	0.725	$61\nu^{as}(CN) - 10\beta(N_1-H_7)$	1156,[39] 1154[39]
13	A′	1047.5	1038.3	1039.6	53.2	0.5	0.534	$53\beta_1(R) - 17\nu(C_5-Br_{11}) + 14\nu(B)$	1055,[c,38] 906, [38] 1048[39]
14	A′	964.0	962.6	961.2	13.1	2.7	0.671	$54\nu_1(R)$	900[39]
15	A′	nd	758.6	771.0	3.0	22.2	0.097	$57\nu(B) - 23\beta_1(R)$	714,[38] 755[39]
16	A′	623.0	622.6	630.2	40.1	0.8	0.555	$49\beta_2(R) - 23\nu(C_5-Br_{11})$	626,[38] 653[39]
17	A′	nd	594.5	601.5	2.1	5.6	0.372	$75\beta^{s}(C=O)$	532,[38] 534[39]
18	A′	531.5	529.6	541.0	9.3	3.9	0.318	$66\beta_3(R)$	594,[38] 564[39]
19	A′	or	395.5	408.4	20.5	2.1	0.594	$59\beta^{as}(C=O) + 14\nu_3(M)$	
20	A′	or	283.4	301.3	1.3	3.5	0.354	$46\nu(C_5-Br_{11}) + 28\beta_2(R)$	
21	A′	or	182.5	202.4	0.8	1.0	0.738	$83\beta(C_5-Br_{11})$	
					Out-of-Plane Modes				
22	A″	900.0	905.8	902.2	15.6	1.8	0.750	$93\gamma(C_6-H_{12})$	962,[38] 964[39]
23	A″	756.0	772.3	775.0	66.7	0.5	0.750	$62\gamma(C_4=O_{10}) + 15\gamma(C_2=O_8)$	760,[38] 622[39]
24	A″	751.0	758.2	760.8	15.7	0.3	0.750	$80\gamma(C_2=O_8) - 17\gamma(C_4=O_{10})$	753,[38] 751[39]
25	A″	656.5	667.8	676.6	64.9	2.2	0.750	$85\gamma(N_3-H_9)$	656,[38] 550[39]
26	A″	547.5	554.3	572.3	58.8	0.7	0.750	$92\gamma(N_1-H_7)$	548,[38] 656[39]
27	A″	or	387.0	397.7	22.1	1.6	0.750	$71\gamma_1(R) + 12\gamma(C_4=O_{10})$	
28	A″	or	271.2	286.2	0.2	0.0	0.750	$89\gamma(C_5-Br_{11})$	
29	A″	or	149.9	171.8	1.1	0.1	0.750	$88\gamma_2(R)$	
30	A″	or	87.7	111.8	1.1	0.4	0.750	$84\gamma_3(R)$	

[a] Calculated frequencies are scaled[62] by the straight line $\nu_{scal} = 0.954\nu_{calc} + 27.6$; I_{IR} stands for IR intensities (km mol^{-1}), R_A denotes Raman activities (Å amu^{-1}), and ρ stands for the depolarization ratio. For local mode definitions, see Table 1S in the Supporting Information. [b] FR denotes involvement of the band in a Fermi resonance, nd stands for not determined, and or stands for out of range. [c] In ref 38, the band is assigned to a ring-stretching mode.

vibrations region. [31] Therefore, one may suppose that a N_3-H_9 vibrations mode is one of the two modes contributing to the combination tone that resonates with a ν(C═O) mode. The sole A′ symmetry N_3-H_9 mode is the $\beta(N_3-H_9)$ mode, whose band is located at ca. 1375 ± 10 cm^{-1} (Table 6). Assuming that the anharmonicity of a combination tone decreases by ca. 50 cm^{-1}, the second mode, which can eventually compose the combination tone absorbing in the C═O stretching region, has a frequency equal to those of the bending β^{as}(C═O) vibrations located at ca. 410 cm^{-1} (Table 6). Another combination that could be taken into account to elucidate the origin of the FR is the sum of the ν_2(R) and β^{s}(C═O) modes, the former located at ca. 1185 cm^{-1} and the latter from 632 to 595 cm^{-1} for the FU and IU molecules, respectively. This hypothesis ignores the influence of N_3-atom substitution on the complexity of the C═O stretching vibrations region, yet it can possibly explain why the middle C═O band shifts from ca. 1740 to 1720 cm^{-1}, for the FU and IU molecules, respectively. The third probable hypothesis could assign the combination tone to the sum of the ring-stretching ν_1(R) and ring-breathing ν(B) modes, located at ca. 960 and 770 cm^{-1}, respectively. However, such a sum would absorb at ca. 1730 cm^{-1} and, to resonate with the ν(C═O) mode, should have a negligible anharmonic component. In conclusion, from among the three above hypotheses about the origin of the FR in the C═O stretching vibrations region in 5-halouracil IR spectra, the most reasonable is the one that assigns the $\beta(N_3-H_9) + \beta^{as}$(C═O) combination tone as resonating with a ν(C═O) mode because only this hypothesis can explain the earlier experimental findings.[30−32,37]

The above hypotheses can be verified partially by calculations of the anharmonic frequencies accompanied by the calculated FRs.[57] Table 6 lists all of the B3PW91/6-311G**-calculated FRs that occur in the ν(C═O) stretching vibrations region. Table 6 shows that the FR in halouracils is quite a complex phenomenon, which probably cannot be explained by assuming only one single resonance mechanism to be operable for all of the molecules. Most of the FRs, in the ν(C═O) stretching vibrations region of halouracils, engage the $\nu(C_4=O_{10})$ mode,

TABLE 5: Bands Observed (ν_{exp}, cm^{-1}) in the Ar-Matrix IR Spectrum of IU Compared with the B3PW91/6-311G-Calculated Wavenumbers (ν_{anh}, ν_{scal}, cm^{-1}) Interpreted in Terms of the PEDs (in Percentages Not Lower than 10%)[a]**

	sym	ν_{exp}[b]	ν_{anh}	ν_{scal}	I_{IR}	R_A	ρ	% PED
				In-Plane Modes				
1	A′	3470.0	3486.5	3514.0	123.8	122.1	0.235	$100\nu(N_1-H_7)$
2	A′	3426.0	3441.4	3476.4	78.9	98.7	0.286	$100\nu(N_3-H_9)$
3	A′	nd	3080.9	3102.0	0.5	62.3	0.361	$99\nu(C_6-H_{12})$
4	A′	1765.5 FR, 1761.5 FR	1814.1	1792.4	803.9	19.1	0.232	$75\nu(C_2=O_8)$
5	A′	1722.5 FR, 1706.5 FR	1765.0	1749.6	420.9	23.9	0.383	$84\nu(C_4=O_{10})$
6	A′	*c*	1636.0	1619.7	90.9	55.9	0.177	$68\nu(C_5=C_6) - 12\beta(C_6-H_{12})$
7	A′	1453.0	1458.0	1458.0	85.4	11.8	0.549	$45\beta(N_1-H_7) + 14\nu_2(R) - 11\nu(C_2=O_8)$
8	A′	1392.5	1374.7	1378.1	57.9	3.2	0.687	$42\beta(N_3-H_9) + 24\nu_3(M)$
9	A′	1384.0	1373.4	1368.5	88.6	0.4	0.674	$30\beta(N_3-H_9) - 25\nu_3(M) - 20\beta(N_1-H_7) + 11\beta^{as}(C=O)$
10	A′	1328.0	1316.5	1314.7	13.2	20.0	0.321	$54\beta(C_6-H_{12}) + 14\nu(C_5=C_6) + 11\nu_2(R)$
11	A′	1189.5, 1186.0	1173.4	1174.6	87.0	1.8	0.666	$48\nu_2(R) - 17\beta(C_6-H_{12}) - 11\beta(N_1-H_7)$
12	A′	1149.0	1140.9	1145.6	19.7	2.4	0.697	$61\nu^{as}(CN) + 11\beta(N_1-H_7)$
13	A′	1029.5	1020.3	1019.6	37.6	1.0	0.448	$56\beta_1(R) + 16\nu(B) - 13\nu(C_5-I_{11})$
14	A′	964.5	962.9	961.7	12.5	3.0	0.726	$55\nu_1(R)$
15	A′	nd	755.7	769.6	1.5	26.2	0.107	$61\nu(B) - 19\beta_1(R)$
16	A′	607.5	606.3	614.0	27.9	1.5	0.673	$53\beta_2(R) - 14\nu(C_5-I_{11})$
17	A′	nd	587.4	595.1	8.3	4.9	0.266	$70\beta^{s}(C=O)$
18	A′	nd	530.4	540.0	10.5	4.2	0.286	$60\beta_3(R)$
19	A′	or	393.1	407.8	21.1	1.7	0.634	$62\beta^{as}(C=O) + 17\nu_3(M) - 11\nu^{as}(CN)$
20	A′	or	239.9	258.1	1.7	4.3	0.324	$57\nu(C_5-I_{11}) + 20\beta_2(R)$
21	A′	or	158.0	178.3	1.6	0.9	0.750	$85\beta(C_5-I_{11})$
				Out-of-Plane Modes				
22	A″	904.0	901.1	907.9	13.3	1.8	0.750	$92\gamma(C_6-H_{12})$
23	A″	756.5	771.5	775.7	66.2	0.6	0.750	$60\gamma(C_4=O_{10}) + 17\gamma(C_2=O_8)$
24	A″	752.5	758.7	761.0	14.0	0.3	0.750	$78\gamma(C_2=O_8) - 19\gamma(C_4=O_{10})$
25	A″	657.5	657.8	678.1	66.3	2.1	0.750	$85\gamma(N_3-H_9)$
26	A″	551.0	563.4	577.6	57.3	0.8	0.750	$92\gamma(N_1-H_7)$
27	A″	or	385.0	399.6	21.7	1.6	0.750	$70\gamma_1(R) + 12\gamma(C_4=O_{10})$
28	A″	or	252.9	269.8	0.6	0.0	0.750	$90\gamma(C_5-I_{11})$
29	A″	or	150.0	171.0	1.0	0.1	0.750	$88\gamma_2(R)$
30	A″	or	81.3	105.9	0.9	0.5	0.750	$87\gamma_3(R)$

[a] Calculated frequencies are scaled[62] by the straight line $\nu_{scal} = 0.954\nu_{calc} + 27.6$; I_{IR} stands for IR intensities (km mol^{-1}), R_A denotes Raman activities (Å amu^{-1}), and ρ stands for the depolarization ratio. For local mode definitions, see Table 1S in the Supporting Information. [b] FR denotes involvement of the band in a Fermi resonance, nd stands for not determined, and or stands for out of range. [c] Band is overlapped by a water-traces band at 1624 cm^{-1}.

and in only 2 of the 15, namely, one for the ClU molecule and one for BrU molecule, is the $\nu(C_2=O_8)$ mode participating. For each halouracil molecule, there is at least one resonance in which the participating mode includes a significant contribution of a β(N−H) mode, and except for FU, it is the $\beta(N_3-H_9)$ mode. Except for the FU molecule, the other mode from the combinational tone is either the β^{as}(C=O) (most often) or the β^{s}(C=O) mode. In the combinational tone, there is often an important contribution of the ν_3(M) and ν^{as}(CN) modes. For the FU, ClU, and BrU molecules, there are resonances with an important contribution of the $\nu(C_5-X_{11})$ mode. A more complete verification of the suggestions resulting from Table 6 would require a comparison of the experimental spectra of diverse deuterated halouracils as well as ^{13}C-, ^{15}N-, and ^{18}O-substituted halouracils; however, there is no report on measurements of the IR spectra of isotopically substituted halouracils, so far, and such a task goes far beyond the scope of the present study.

ν(C=C) Stretching Vibrations. *DFT Calculations.* The scaled harmonic frequency calculations predict the $\nu(C_5=C_6)$ band to shift toward lower wavenumbers with an increase in the halogen mass from ca. 1680 cm^{-1} for FU to ca. 1620 cm^{-1} for IU (Tables 1−5). For unsubstituted uracil, the band is calculated to occur at ca. 1640 cm^{-1}, a position that agrees very well with the literature value of 1643 cm^{-1}.[30] Again, the anharmonic frequencies are higher than the scaled harmonic ones by ca. 15 cm^{-1}. The PED analysis suggests that the ν(C=C) mode is ca. 70% pure ν(C=C) vibration. This means that the ν(C=C) vibrations are coupled to the ν(C=O) modes for a value of, at most, 30%. Unlike the band frequency, the IR intensity is predicted to increase with the halogen mass from ca. 35 km/mol for FU to ca. 90 km/mol for IU, and unsubstituted uracil is predicted to have a value between these two limits (Tables 1−5).

Ar-Matrix IR Spectra. The positions of the C=C stretching vibrations bands in the experimental spectra of halouracils are in agreement with those in the theoretical prediction (Tables 1−5). In the case of unsubstituted uracil, the band (at 1643 cm^{-1}; ref 30) appeared too weak to be detected in the measured spectra, and in the case of IU, it was overlapped by a water-traces band at 1624 cm^{-1} (Tables 1 and 5).

β(N−H) Bending Vibrations. *DFT Calculations.* According to the calculations, there are three modes to which the β(N−H) bending vibrations contribute significantly: $\beta(N_1-H_7)$, ν_3(M) + $\beta(N_3-H_9)$, and $\beta(N_3-H_9)$, positioned at ca. 1465, 1380, and 1370 cm^{-1}, respectively (Tables 1−5; Figure 3). In one case, that is, the FU molecule, the ν_3(M) vibrations couple with the $\beta(N_1-H_7)$ mode rather than the $\beta(N_3-H_9)$ mode. Despite the fact that the PED contribution of the β(N−H) mode usually does not exceed 45% (Tables 1−5), we continue to use the above notation of the bands. For these modes, the anharmonic frequencies are in concordance with the scaled harmonic ones. As the halogen mass is increased, the $\beta(N_1-H_7)$ and

TABLE 6: Modes Supposed To Be Engaged in FRs with the ν(C=O) Modes [ν_1 and ($\nu_2 + \nu_3$)] in 5-Halouracils According to the Anharmonic Frequency DFT/B3PW91/6-311G Calculations[a]**

	ν_1		$f_{1,2,3}$	$\nu_2+\nu_3$	ν_2		ν_3	
HU	$77\nu(C_4{=}O_{10})$	1785.2	6.955	1774.7	$69\beta^{as}(C{=}O) - 15\nu_3(M)$	388.8	$31\nu_3(M) - 25\beta(N_3{-}H_9) + 20\beta(C_6{-}H_{12})$	1385.9
	$77\nu(C_4{=}O_{10})$	1785.2	1.137	1767.1	$69\beta^{as}(C{=}O) - 15\nu_3(M)$	388.8	$43\beta(N_3{-}H_9) + 12\nu_3(M) - 12\beta(N_1{-}H_7)$	1378.3
FU	$78\nu(C_4{=}O_{10})$	1785.5	−10.500	1779.2	$61\beta_3(R)$	530.3	$44\nu(C_5{-}F_{11}) + 14\nu_3(M) + 14\beta_1(R)$	1248.9
	$78\nu(C_4{=}O_{10})$	1785.5	−0.632	1773.6	$76\beta_2(R)$	449.7	$46\beta(C_6{-}H_{12}) + 16\nu_2(R) + 11\nu_1(R)$	1323.9
	$78\nu(C_4{=}O_{10})$	1785.5	−6.822	1772.1	$81\beta(C_5{-}F_{11})$	300.4	$31\beta(N_1{-}H_7) - 19\nu_3(M) + 13\nu_2(R)$	1471.7
ClU	$74\nu(C_2{=}O_8)$	1811.5	6.366	1807.7	$37\beta_2(R) - 31\nu(C_5{-}Cl_{11}) - 14\nu(B)$	656.9	$58\nu^{as}(CN) - 10\beta(N_1{-}H_7)$	1150.8
	$82\nu(C_4{=}O_{10})$	1783.2	13.160	1773.9	$73\beta^{s}(C{=}O)$	604.1	$46\nu_2(R) - 20\beta(C_6{-}H_{12}) - 11\beta(N_1{-}H_7)$	1169.8
	$82\nu(C_4{=}O_{10})$	1783.2	−10.328	1775.7	$52\beta^{as}(C{=}O) + 14\nu_3(M) + 10\nu^{as}(CN)$	405.0	$47\beta(N_3{-}H_9) - 17\beta(N_1{-}H_7) - 19\nu_3(M) + 11\beta^{as}(C{=}O)$	1370.7
BrU	$74\nu(C_2{=}O_8)$	1814.2	3.720	1796.9	$57\nu(B) - 23\beta_1(R)$	758.6	$53\beta_1(R) - 17\nu(C_5{-}Br_{11}) + 14\nu(B)$	1038.3
	$83\nu(C_4{=}O_{10})$	1784.9	37.785	1766.9	$49\beta_2(R) - 23\nu(C_5{-}Br_{11})$	622.6	$61\nu^{as}(CN) - 10\beta(N_1{-}H_7)$	1144.3
	$83\nu(C_4{=}O_{10})$	1784.9	9.929	1772.5	$59\beta^{as}(C{=}O) + 14\nu_3(M)$	395.5	$31\nu_3(M) + 34\beta(N_3{-}H_9)$	1377.0
	$83\nu(C_4{=}O_{10})$	1784.9	−5.829	1766.4	$59\beta^{as}(C{=}O) + 14\nu_3(M)$	395.5	$38\beta(N_3{-}H_9) - 19\beta(N_1{-}H_7) - 19\nu_3(M) + 13\beta^{as}(C{=}O)$	1370.9
IU	$84\nu(C_4{=}O_{10})$	1765.0	−2.371	1760.8	$70\beta^{s}(C{=}O)$	587.4	$48\nu_2(R) - 17\beta(C_6{-}H_{12}) - 11\beta(N_1{-}H_7)$	1173.4
	$84\nu(C_4{=}O_{10})$	1765.0	−10.536	1767.8	$62\beta^{as}(C{=}O) + 17\nu_3(M) - 11\nu^{as}(CN)$	393.1	$42\beta(N_3{-}H_9) + 24\nu_3(M)$	1374.7
	$84\nu(C_4{=}O_{10})$	1765.0	−2.936	1766.5	$62\beta^{as}(C{=}O) + 17\nu_3(M) - 11\nu^{as}(CN)$	393.1	$30\beta(N_3{-}H_9) - 25\nu_3(M) - 20\beta(N_1{-}H_7)$	1373.4

[a] $f_{1,2,3}$ stands for the *ijk* force constant (cm^{-1}), the sign of which denotes the character of its contribution to the anharmonic energy term.[58] Modes are interpreted according to PED analysis (Tables 1−5).

$2\nu_3(M) + \beta(N_3{-}H_9)$ mode frequencies are predicted to decrease slightly. For uracil, the β(N−H) local vibrations couple to the β(C−H) modes and form a complicated spectral pattern (Table 1; Figure 3). The IR intensities of the $\beta(N_1{-}H)$ and $\beta(N_3{-}H)$ modes tend to increase from FU to IU, while at the same time, the intensity of the $\nu_3(M) + \beta(N_3{-}H_9)$ mode remains almost constant. The Raman activity of the $\beta(N_1{-}H)$ mode of 5-halouracil molecules is ca. 10 times greater than that of the $\beta(N_3{-}H)$ mode (Tables 2−5), and that of the $\beta(N_3{-}H_9)$ mode decreases as the substituent mass is increased. The Raman activity of the $\nu_3(M) + \beta(N_3{-}H_9)$ mode is between those of the two other β(N−H) vibrations (Tables 2−5).

Ar-Matrix IR Spectra. The positions of the β(N−H) modes in the matrix isolation IR spectra of the halouracil molecules are in line with those of the theoretical results (Figure 3). In contrast to the DFT prediction, the IR intensity of the $\beta(N_3{-}H_9)$ band is much lower than those of the $\nu_3(M) + \beta(N_3{-}H_9)$ and $\beta(N_1{-}H_7)$ bands (Figure 3). However, the calculated band intensities are usually less reliable than the band frequencies. The decrease of the band frequency predicted to take place with the increase in the halogen mass is valid for the $\beta(N_1{-}H_7)$ band only.

Our assignment of the $\beta(N_1{-}H_7)$ band in the low-temperature IR spectra of uracil and halouracils is in agreement with most of the literature data;[29−38] some investigators have assigned the $\beta(N_1{-}H_7)$ mode to the band positioned at ca. 100 cm^{-1} wavenumbers lower.[39]

The $\beta(N_3{-}H_9)$ mode contributes mainly to two modes, $\beta(N_3{-}H_9)$ and $\nu_3(M) + \beta(N_3{-}H_9)$, yet for uracil itself, it contributes to some other vibrations. For example, Ivanov et al.[36] have assigned the $\beta(N_3{-}H_9)$ modes in uracil to be the $\beta(N_3{-}H) + \nu(C_2{-}N_3)$ and $\beta(N_3{-}H) + \nu(N_3{-}C_4)$ modes, which differ in position by ca. 10 cm^{-1}, whereas the uracil band at 1399 cm^{-1} has been referred to by Barnes et al. as the "ring str/NH bend" and those at 1389 and 1386 cm^{-1} as the "CH/NH i.p. bend".[32] However, in most cases, the various modes to which the $\beta(N_3{-}H_9)$ mode contributes have not been discerned. This is why, for this region of spectra, some differences may occur in the interpretations.[29−39]

$\beta(C_6{-}H_{12})$ Bending Vibrations. *DFT Calculations.* For 5-halouracils, the $\beta(C_6{-}H_{12})$ mode frequency is predicted to occur at ca. 1315 cm^{-1} (Tables 2−5). The analogous band in uracil is predicted to occur at 1350 cm^{-1} and to be coupled with the ring-stretching ν_2(R) mode (Table 1). The theoretical IR intensity of the $\beta(C_6{-}H_{12})$ mode changes irregularly while the Raman activity is expected to decrease slightly as the halogen mass is increased (Tables 1−5).

Ar-Matrix Spectra. The Ar-matrix $\beta(C_6{-}H_{12})$ bands are located at ca. 1330 cm^{-1}, and except for FU, they exhibit quite low intensities (Figure 3). The $\beta(C_6{-}H_{12})$ band of uracil can be found at 1359 cm^{-1}. The low intensity of the band may be a reason other investigators have assigned the band at 1182 cm^{-1} for FU[38] and that at 1192 [38] or 1189 cm^{-1} [39] for BrU. At the same time, our assignment of the $\beta(C_6{-}H_{12})$ band of uracil in low-temperature matrixes is in good agreement with the assignments proposed in refs 36 and 38, whereas the assignments given in refs 29, 30, 32, 33, 35, and 37 correspond to the band assigned here to the $\nu_3(M) + \beta(N_3{-}H_9)$ mode. Moreover, in ref 31, the assignments of the $\beta(C_6{-}H_{12})$ and $\beta(C_5{-}H_{11})$ bands are interchanged.

$\beta(C_5{-}X_{11})$ Bending Vibrations. *DFT Calculations.* The theoretical prediction of the $\beta(C_5\text{-}X_{11})$ bending vibration frequencies shows a systematic decrease on passing from the FU to the IU molecule (Tables 2−5). Obviously, the analogous C−H bending vibrations band of the uracil molecule is

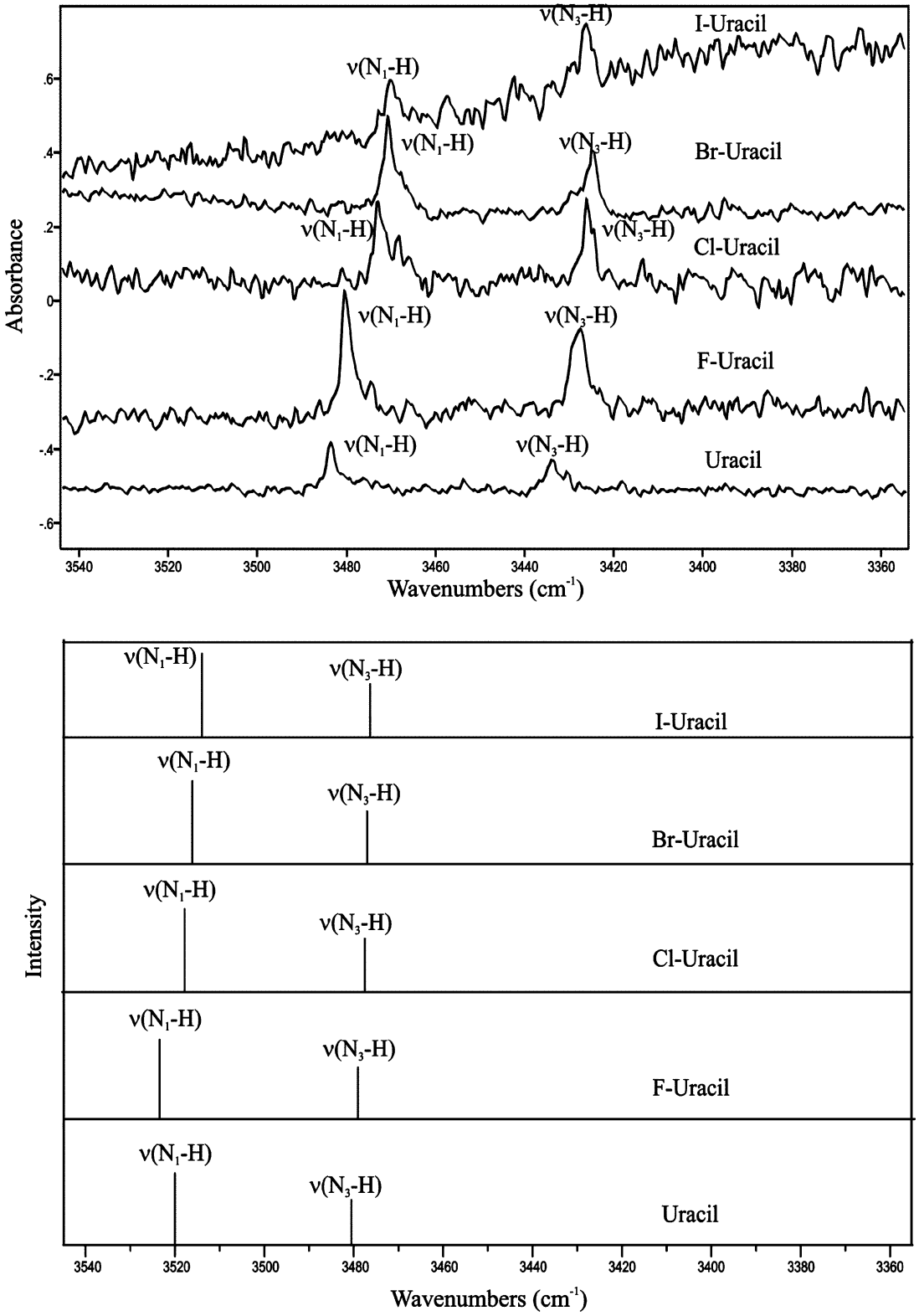

Figure 1. Experimental Ar-matrix low-temperature FTIR spectra (top) and B3PW91/6-311G**-calculated scaled harmonic vibrations (bottom) of uracil and its halo derivatives in the range of 3350−3550 cm^{-1}.

2positioned at ca. 1200 cm^{-1} (Table 1). The theoretical IRintensity of the $\beta(C_5-X_{11})$ mode increases and the Raman activity decreases from ClU to IU (Tables 2−5).

Ar-Matrix Spectra. The low-frequency limit of our Ar-matrix FTIR spectra was 400 cm^{-1}. Therefore, we can assign solely the $\beta(C_5-H_{11})$ band of uracil at 1217 cm^{-1} (Table 1). Our assignment is identical with those given by Szczepaniak et al.,[30] Barnes et al.,[32] and Maltese et al.[37] and different from the assignments made by Nowak,[29] Graindourze et al.,[31,38] Szczesniak et al.,[33] and Ivanov et al.[36]

ν_2(R) Stretching Vibrations. *DFT Calculations.* The ν_2(R) ring-stretching vibration, defined in Table 1S in the Supporting Information, is predicted to occur between 1160 and 1175 cm^{-1}. The ν_2(R) local mode explains only 50% of the vibration (Tables 1−5). The IR intensity of the band is moderate and is practically not affected by substitution at the C5 atom.

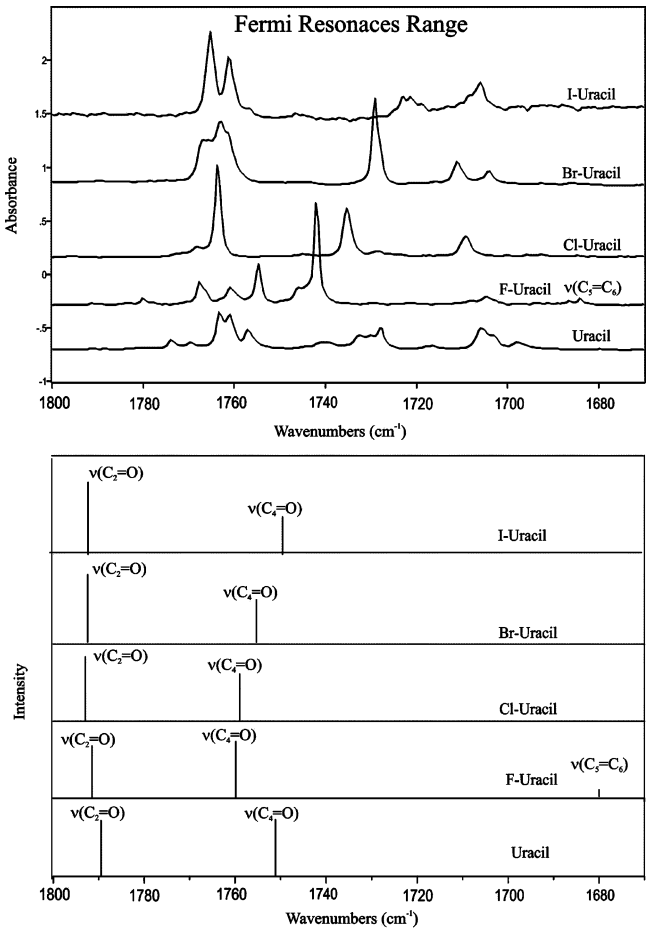

Figure 2. Experimental Ar-matrix low-temperature FTIR spectra (top) and B3PW91/6-311G**-calculated scaled harmonic vibrations (bottom) of uracil and its halo derivatives in the range of 1670−1800 cm^{-1}.

Ar-Matrix Spectra. The experimental ν_2(R) IR band is localized at frequencies higher, by ca. 10 cm^{-1}, than those predicted by calculations (Tables 1−5).

ν^{as}(CN) Stretching Vibrations. *DFT Calculations.* For halouracils, the ν^{as}(CN) vibrations are predicted to occur at 1150 ± 10 cm^{-1}, to have PEDs equal to ca. 60%, and to mix slightly with the $\beta(N_1-H_7)$ mode (Tables 2−5). The local ν^{as}(CN) mode in unsubstituted uracil contributes significantly to two normal modes predicted to be positioned at ca. 1200 cm^{-1} [assigned here as the $\beta(C_5-H_{11})$ mode] and ca. 1070 cm^{-1} [assigned here as the ν^{as}(CN) vibration], to which the $\beta(C_5-H_{11})$ and $\beta(N_1-H_7)$ local vibrations also contribute.

Ar-Matrix Spectra. The positions of the experimental bands agree quite well with the theoretical predictions; however, the scaled harmonic frequencies fit the experimental bands just slightly better than the anharmonic ones (Tables 1−5).

β_1(R) Bending Vibrations. *DFT Calculations*. According to the calculations followed by the PED analysis, the β_1(R) ring-bending vibrations modes are located at ca. 1070, 1040, and 1020 cm^{-1} for the ClU, BrU, and IU molecules, respectively (Tables 3−5), whereas for the FU and unsubstituted uracil molecules, they are located at ca. 810 and 980 cm^{-1}, respectively (Tables 2 and 1). Such radical frequency changes are probably due to a significant contribution of the $\nu(C_5-X_{11})$ local mode in the normal mode of halouracils and that of the ν(B) vibrations in uracil. The band is of moderate IR intensity, except for that of uracil, for which it is rather weak (Figure 4). The Raman activity is predicted to be weak (Tables 1−5).

Ar-Matrix Spectra. The experimental bands assigned to the β_1(R) ring-bending vibrations mode are located at 1073, 1048, 1029, 807, and 983 cm^{-1} for the ClU, BrU, IU, FU, and uracil molecules, respectively (Tables 1−5). Because of the small intensity of the $\beta(R_1)$ band of uracil, its assignment can be questioned (Figure 4; Table 1). Only two papers have mentioned the ring bendings of halouracils.[38,39] However, Graindourze et al. assigned the ring bending to 876 cm^{-1} for FU and to 906 cm^{-1} for BrU, while the bands at 807 cm^{-1} in the FU spectrum and at 1055 cm^{-1} in the BrU spectrum were assigned to the C−F stretching and ring stretching, respectively.[38] The assignment made by Stepanian et al.[39] for the BrU molecule is identical with that of this paper. The literature assignments for the uracil molecule are spread out within a small interval of 960−990 cm^{-1} (close to our calculated value of 976 cm^{-1}), and it is difficult to judge which assignment is correct.[29−33,36]

ν_1(R) Stretching Vibrations. *DFT Calculations*. The ν_1(R) ring-stretching vibration, defined here as the antisymmetric stretching of the opposite C_4-C_5 and N_1-C_2 bonds (Table 1S in the Supporting Information), is predicted to occur near 960 cm^{-1}. Although the ν_1(R) local mode explains only ca. 50% of the normal vibration, the other local vibrations contribute to this mode to an extent smaller than 10% for each (Tables 1−5). The IR intensity of the band is moderate and, similarly to the mode frequency, is practically not affected by substitution at the C5 atom.

Ar-Matrix Spectra. The experimental ν_1(R) IR bands are localized at wavenumbers almost identical with those predicted by calculations (Figure 4; Tables 1−5).

ν(B) Ring-Breathing Vibrations. *DFT Calculations*. The ν(B) ring-breathing vibrations are predicted to occur at 760 ± 10 cm^{-1}, except for that of FU, which is localized at ca. 735 cm^{-1} (Figure 4). The calculations indicate that its IR intensity should be weak, while the Raman intensity is expected to be significant (Tables 1−5). The ν(B) local mode explains, again, ca. 50% of the normal vibrations that also have a significant contribution to the $\beta(R_1)$ mode.

Ar-Matrix Spectra. Because of small intensities, the experimental IR ν(B) bands were not detected in our spectra.

β_2(R) Bending Vibrations. *DFT Calculations*. The β_2(R) ring-bending mode is the only local mode whose definition changes with halogen substitution (Table 1S in the Supporting Information); however, antisymmetric $\beta(N_3-C_4-C_5)-\beta(N_1-C_2-N_3)$ bending is common for all of those definitions. For the ClU, BrU, and IU molecules, the β_2(R) mode couples with the ν(C−X) vibration (Figure 5). This is why, for the ClU, BrU, and IU molecules, the mode is predicted to occur at ca. 660, 625, and 610 cm^{-1}, respectively, whereas for the FU and uracil molecules, in which it is practically uncoupled with other local modes, it is located at ca. 450 and 520 cm^{-1}, respectively (Tables 1−5). The mode is of moderate IR intensity, except for FU, where it is much weaker (Figure 5). The Raman activity is predicted to be weak (Tables 1−5).

Ar-Matrix Spectra. The β_2(R) band is easily detectable in the FTIR Ar-matrix spectra for the ClU, BrU, IU and uracil molecules (Figure 5), whereas for FU, there is a weak-intensity band at 451 cm^{-1} (Figure 5; Table 2). The β_2(R) band was previously reported only for BrU: Graindourze et al.[38] assigned the β_2(R) band at 626 cm^{-1}, in good agreement with our assignment, while Stepanian et al.[39] assigned it at 653 cm^{-1}.

β^s(C=O) and β^{as}(C=O) Bending Vibrations. *DFT Calculations*. According to the PED analysis, the sum of the two local modes, $\beta(C_2=O_8)$ and $\beta(C_4=O_{10})$, is the dominating contribution to the mode absorbing at ca. 630, 605, 600, and 590 cm^{-1} for the FU, ClU, BrU, and IU molecules, respectively (Tables 2−5). The analogous uracil mode is predicted to absorb at ca.

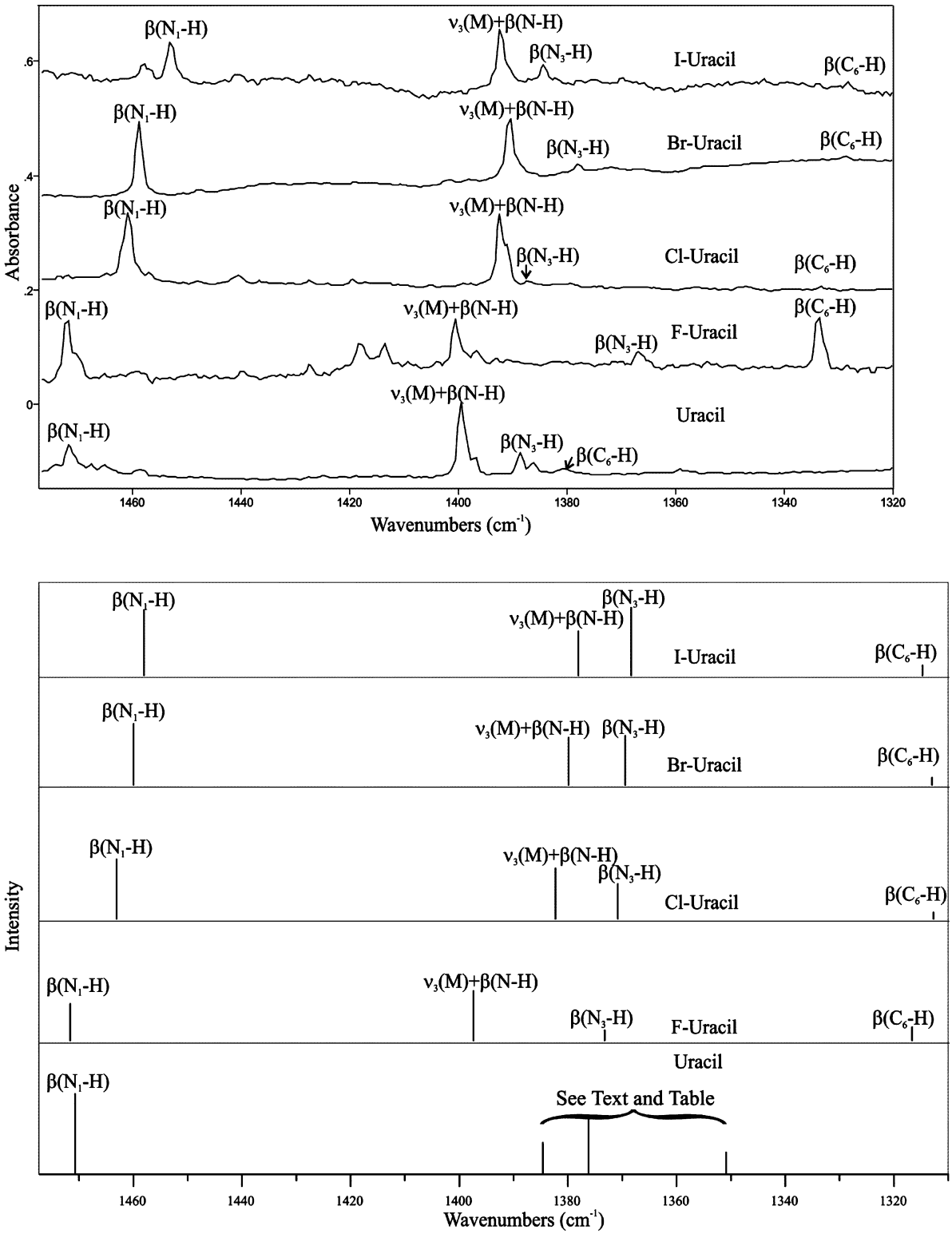

Figure 3. Experimental Ar-matrix low-temperature FTIR spectra (top) and B3PW91/6-311G**-calculated scaled harmonic vibrations (bottom) of uracil and its halo derivatives in the range of 1320−1470 cm^{-1}.

555 cm^{-1}. The theoretical IR intensity of the mode is weak for all of the spectra studied, and for ClU, it is practically inactive (Table 3). The theoretical Raman activity of the mode is moderate.

According to the PED analysis, the difference of the two local β(C═O) modes contributes to the band at ca. 400 cm^{-1}, with a PED value of ca. 60% (Tables 1−5). The theoretical IR intensity of the band is moderate, while the Raman activity is rather weak.

Ar-Matrix Spectra. The low intensity of the β^{s}(C═O) band is the reason we, and other investigators,[29,38,39] have had difficulties in assigning the band in halouracil spectra. For uracil, our assignment agrees with that in ref 30, although others have assigned the β^{s}(C═O) mode to the band located at ca. 536 cm^{-1}.[29−33,36−38]

Because of the low-frequency limit of our Ar-matrix IR spectra (400 cm^{-1}), we did not assign the β^{as}(C═O) band. The

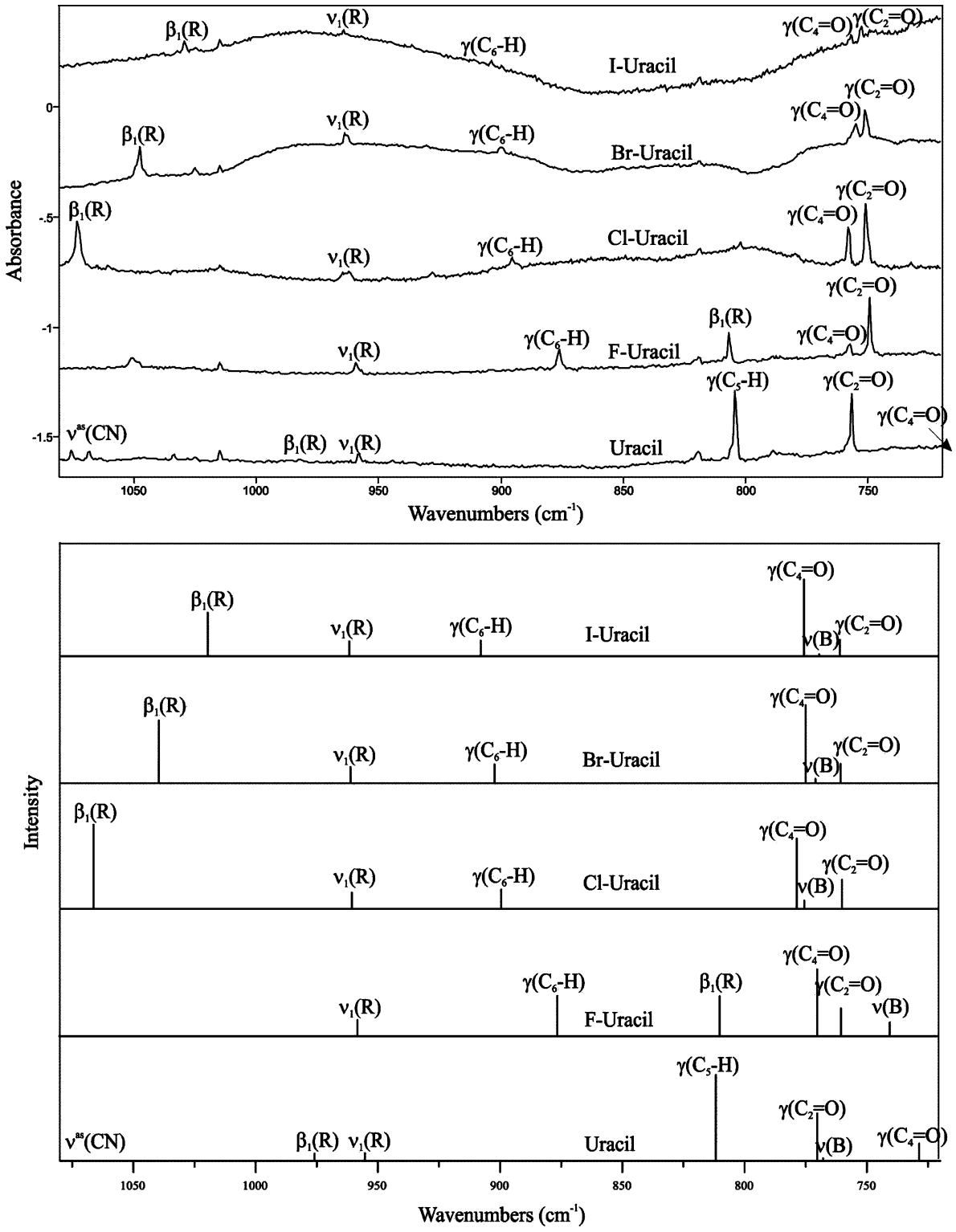

Figure 4. Experimental Ar-matrix low-temperature FTIR spectra (top) and B3PW91/6-311G**-calculated scaled harmonic vibrations (bottom) of uracil and its halo derivatives in the range of 720−1080 cm^{-1}.

literature assignments of the band in uracil and FU spectra are in line with our calculations (Tables 1 and 2).[29,30]

β_3(R) Bending Vibrations. *DFT Calculations.* The β_3(R) ring-deformation mode, defined in Table 1S in the Supporting Information, is predicted to occur at ca. 540 cm^{-1} (Figure 5). The calculated intensity of the IR absorption increases from the FU to the IU molecule, whereas the calculated activity of Raman scattering is more or less constant (Tables 1−5).

Ar-Matrix Spectra. In the experimental spectra, the β_3(R) band is located close to the predicted position, that is, at ca. 530 cm^{-1}. In the case of IU, the noise of the spectrum is large and the assignment is vague. There are two literature assignments of the ring-deformation band in a similar region for the BrU molecule: at 594 [38] and 564 cm^{-1}.[39] However, in our BrU spectrum, there are no bands at those wavenumbers. For uracil, the reported assignments[29−33,36,37] are in line with our assignment.

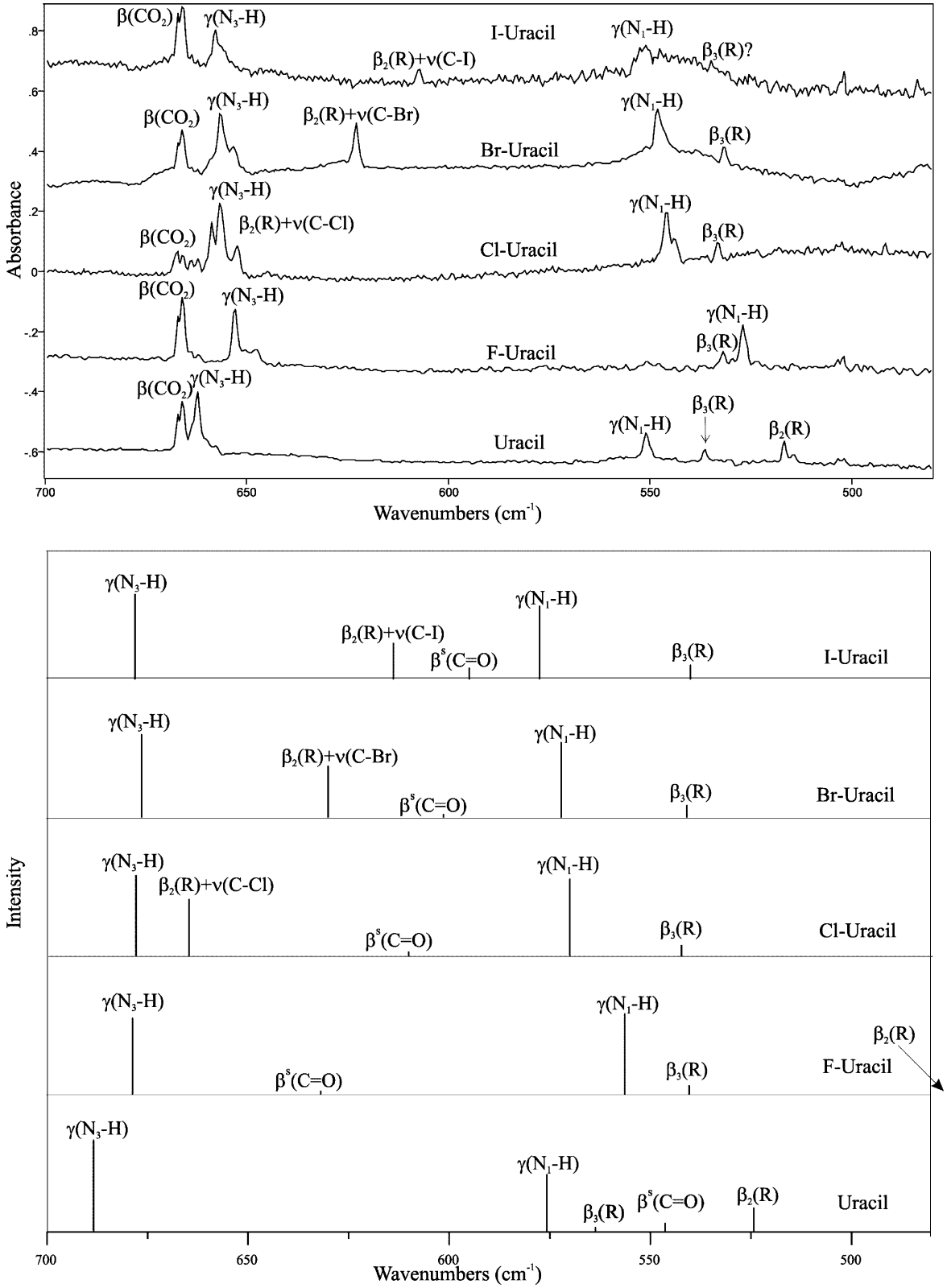

Figure 5. Experimental Ar-matrix low-temperature FTIR spectra (top) and B3PW91/6-311G**-calculated scaled harmonic vibrations (bottom) of uracil and its halo derivatives in the range of 475−700 cm^{-1}.

$\gamma(C_6-H_{12})$ Out-of-Plane Vibrations. *DFT Calculations*. For halouracils, the out-of-plane $\gamma(C_6-H_{12})$ vibrations mode is predicted to occur in the range of 875−905 cm^{-1} and to increase on passing from FU to IU, whereas for uracil, it is predicted to occur at ca. 950 cm^{-1} (Figure 4). The theoretical IR intensity of the mode is of moderate intensity and decreases on passing from FU to IU, whereas for uracil, the mode is predicted to be almost inactive. The Raman activity of the mode is moderate (Tables 1−5).

Ar-Matrix Spectra. The assignment of the $\gamma(C_6-H_{12})$ vibrations band in the Ar-matrix spectra is in very good agreement with our DFT calculations (Figure 4; Tables 1−5). However, in the case of the uracil spectrum, the band was not assigned because it was weak and probably overlapped by the ν_1(R) band.

Again, there are only a few assignments for this band in halouracils,[38,39] and in our opinion, they are erroneous: the bands are assigned to ca. 960 cm^{-1}, the place where the ν_1(R) stretching vibrations absorb (Figure 4; Tables 2 and 4). Moreover, some authors assign the $\gamma(C_6-H_{12})$ vibrations band of uracil to the absorption at ca. 985 cm^{-1},[29,31,36] one assigns it to the band at ca. 944 cm^{-1},[30] and one assigns it to the band at 842 cm^{-1}.[32] On the basis of our calculations, we see a possibility that the assignment to the small band at 944 cm^{-1} is correct,[30] yet the other assignments for the $\gamma(C_6-H_{12})$ vibrations seem, to us, improbable because, in this very place, the β_1(R) band is positioned (Figure 4; Table 1).

γ(N−H) Out-of-Plane Vibrations. *DFT Calculations*. For uracil and halouracils, the $\gamma(N_3-H_9)$ out-of-plane vibrations mode is predicted to occur at ca. 675 or ca. 660 cm^{-1} for the scaled harmonic or anharmonic approximation, respectively (Figure 5; Table 1−5). The mode is nearly pure $\gamma(N_3-H_9)$, with a PED value of ca. 85%. Its IR intensity is moderate and is supposed to increase slightly on passing from FU to IU, and the Raman activity is predicted to remain unaffected by halogen substitution (Tables 1−5).

The $\gamma(N_1-H_7)$ out-of-plane vibrations mode is a practically pure $\gamma(N_1-H_7)$ vibration with a PED value of 90% and is predicted to occur at ca. 570 or ca. 545 cm^{-1} for the scaled harmonic or anharmonic approximation, respectively (Figure 5; Table 1−5), except for the FU molecule, in which it is calculated to occur at ca. 15 cm^{-1} below those frequencies. A more detailed look into the mode frequency shows that it increases only slightly on passing from FU to IU. The calculated IR intensity of the mode is moderate and slightly decreases from Fu to IU, and the calculated Raman activity is constant (Figure 5; Tables 1−5).

Ar-Matrix Spectra. The $\gamma(N_3-H_9)$ out-of-plane vibrations band is assigned to ca. 655 cm^{-1}, which is close to the $\beta(CO_2)$ bending CO_2 vibrations band at 667 cm^{-1} (Figure 5). For the FU and BrU molecules, the assignments given in refs 29 and 38 are identical with ours, whereas in ref 39, the assignment for BrU is mistaken for that of the $\gamma(N_1-H_7)$ mode. The assignment for the $\gamma(N_3-H_9)$ out-of-plane vibrations band in the uracil spectrum is identical with the previous assignments.[29−33,36−38]

The experimental mode frequency is detected at a frequency lower by ca. 10 cm^{-1} than that predicted by the anharmonic DFT calculations. As suggested by the calculations, the mode frequency increases slightly from FU to IU (Figure 5; Tables 1−5). The $\gamma(N_1-H_7)$ out-of-plane vibrations band was found in the FU[29,38] and BrU[38,39] Ar-matrix spectra. However, for FU, the band was detected at 571 cm^{-1},[29,38] where there is no band in our spectrum (Figure 5). Moreover, the $\gamma(N_1-H_7)$ band in the BrU spectrum[39] is assigned to 656 cm^{-1}, that is, at the position of the $\gamma(N_3-H_9)$ band. Thus, the only correct assignment for the BrU molecule can be found in work by Graindourze et al.[38] (Table 4). The assignment for uracil[29−32,36−38] is in harmony with that given in this paper, whereas out of the two bands (585 and 557 cm^{-1}) assigned in ref 13 to the γ(N−H) mode, the first is absent in our spectrum and the second is probably the same as our $\gamma(N_1-H_7)$ band.

γ(C═O) Out-of-Plane Vibrations. *DFT Calculations*. Unlike for the β(C═O) modes, the two out-of-plane bending vibrations γ(C═O) modes are mixed only slightly. The $\gamma(C_4{=}O_{10})$ mode is predicted to occur at ca. 770 cm^{-1} (Figure 4; Tables 2−5). The analogous uracil mode is predicted to occur at ca. 725 cm^{-1} and has a significant contribution (PED of ca. 20%) in the γ_1(R) mode at ca. 400 cm^{-1} (Table 1). The calculated IR intensity of the $\gamma(C_4{=}O_{10})$ mode is moderate and exhibits a tendency to increase as the halogen mass is increased. The Raman activity is predicted to be weak.

The out-of-plane vibrations $\gamma(C_2{=}O_8)$ mode is predicted to occur at ca. 760 cm^{-1} (Figure 4; Tables 1−5). The theoretical IR intensity tends to decrease from uracil to IU and is predicted to be ca. 2−3 times lower than that of the $\gamma(C_4{=}O_{10})$ mode. The Raman activity is predicted to be almost zero (Tables 1−5).

Ar-Matrix Spectra. The experimental $\gamma(C_4{=}O_{10})$ band is located at ca. 755 cm^{-1} (Figure 4). The band does not appear to be affected by halogen substituents. The assignment by Graindourze et al. for the FU[38] and BrU molecules is similar to that in this paper, whereas that proposed by Nowak for the FU[29] molecules and that by Stepanian et al. for the BrU molecules[39] are different. There is a discrepancy in the literature assignments of the $\gamma(C_4{=}O_{10})$ mode for uracil.[29−33,36,38] Some investigators have assigned the $\gamma(C_4{=}O_{10})$ mode to the band at ca. 805 cm^{-1},[31−33] where, in our opinion, the $\gamma(C_5-H_{11})$ band is positioned, and some, including us, have assigned it to the band at ca. 715 cm^{-1}.[29,30,36]

The experimental $\gamma(C_2{=}O_8)$ band is located at ca. 750 cm^{-1} (Figure 4; Tables 1−5). In contrast to the DFT results, the observed $\gamma(C_2{=}O_8)$ band intensity is ca. half as large as that of the $\gamma(C_4{=}O_{10})$ band (Figure 4). Our assignments for FU and BrU are coherent with the previous predictions of that band in matrix spectra.[29,38,39] For uracil, the assignments given by different authors are in good agreement.[29−33,36,38]

$\gamma(C_5-X_{11})$ Out-of-Plane Vibrations. *DFT Calculations*. The out-of-plane $\gamma(C_5-X_{11})$ vibrations mode is predicted to change its position significantly with an increase in the halogen atom mass from ca. 350 cm^{-1} for FU to 250 cm^{-1} for IU. For ClU, BrU, and IU, the mode is practically IR-inactive, whereas for FU, the $\gamma(C_5-F_{11})$ mode has a rather low IR intensity (Table 2). For halouracils, the Raman activity should be very weak. For uracil, the $\gamma(C_5-H_{11})$ mode should appear as an intense band located at ca. 810 cm^{-1} (Table 1).

Ar-Matrix Spectra. Because of the low-frequency limit of our measurements (400 cm^{-1}), we assigned only the uracil's $\gamma(C_5-H_{11})$ vibrations band at 804 cm^{-1}, as in refs 29, 30, 36, and 37. In the literature, the $\gamma(C_5-H_{11})$ band has also been assigned to the band at 718 cm^{-1},[31,32,38] where, according to our analysis, the $\gamma(C_5-H_{11})$ contributes, though slightly, to the $\gamma(C_4{=}O_{10})$ band.

γ_1(R), γ_2(R), and γ_3(R) Out-of-Plane Vibrations. *DFT Calculations*. Out of the three out-of-plane ring-bending γ(R) modes predicted to occur below 400 cm^{-1}, only the γ_1(R) mode is predicted to appear in the IR spectra (it should be located at ca. 385 cm^{-1}), to have a low intensity, and to contribute somewhat to the $\gamma(C_4{=}O_{10})$ mode (Tables 1−5).

Conclusions

The infrared low-temperature Ar-matrix IR spectra of 5-halouracils and uracil were measured and interpreted in terms of the DFT/B3PW91/6-311G** calculations of scaled harmonic and anharmonic vibrational spectra followed by a PED analysis. A comparison of the set of theoretical and experimental spectra taken for analogous molecules enabled the credibility of the assignments to be increased. The PED analysis performed was based on a set of mode definitions, uniform for all halouracils, enabling the theoretical spectra to be consistently examined.

On the basis of the calculated anharmonic vibrational IR spectra, we demonstrated that the FR in the ν(C═O) region of the halouracil spectra is a complex phenomenon, which probably

cannot be explained by assuming only one resonance mechanism to be responsible for all of the halouracils. Most of the FRs involve the $\nu(C_4{=}O_{10})$ mode. For each halouracil molecule, there is at least one resonance in which a mode participates, endowed with a significant contribution of a β(N−H) mode [usually $\beta(N_3{-}H_9)$]. The other resonance mode from the combinational tone is either the β^{as}(C═O) (most often) or the β^{s}(C═O) mode.

The experimental ν(N−H) frequencies are reproduced by the calculated anharmonic frequencies better than by the scaled harmonic ones; the ν(C═O) frequencies, for which anharmonicity is much weaker, respond in the opposite manner. The experimental frequencies located below 1500 cm^{-1} are reproduced equally well by the two kinds of calculations. Unexpectedly, the only mode for which anharmonicity was induced by going from FU to IU appeared to be the $\nu(C_5{-}X_{11})$ mode.

Acknowledgment. The computational Grant G19-4 from the Interdisciplinary Center of Mathematical and Computer Modeling (ICM) at Warsaw University is gratefully acknowledged.

Supporting Information Available: Table 1S contains definitions of internal coordinates and notation used in the PED analysis of the vibrational modes of uracil and halouracil molecules. Table 2S juxtaposes the band positions (cm^{-1}) in the Ar-matrix IR spectra of 5-halouracils. This material is available free of charge via the Internet at http://pubs.acs.org.

References and Notes

(1) *Basic and Clinical Pharmacology*, 6th ed.; Katzung, B. A., Ed.; Appleton & Lange: Norwalk, CT, 1995.
(2) Longley, D. B.; Harkin, D. P.; Johnston, P. G. *Nat. Rev. Cancer* **2003**, *3*, 330−338.
(3) Argiris, A.; Haraf, D. J.; Kies, M. S.; Vokes, E. E. *Oncologist* **2003**, *8*, 350−60.
(4) Malet-Martino, M.; Jolimaitre, P.; Martino, R. *Curr. Med. Chem.: Anti-Cancer Agents* **2002**, *2*, 267−310.
(5) Bodet, C. A., III; Jorgensen, J. H.; Drutz, D. J. *Antimicrob. Agents Chemother.* **1985**, *28*, 437−439.
(6) Nyhlen, A.; Ljungberg, B.; Nilsson-Ehle, I.; Odenholt, I. *Chemotherapy* **2002**, *48*, 71−77.
(7) Krenitsky, T. A.; Freeman, G. A.; Shaver, S. R.; Beacham, L. M., III; Hurlbert, S.; Cohn, N. K.; Elwell, L. P.; Selway, J. W. *J. Med. Chem.* **1983**, *26*, 891−895.
(8) Verheggen, I.; Van Aerschot, A.; Van Meervelt, L.; Rozenski, J.; Wiebe, L.; Snoeck, R.; Andrei, G.; Balzarini, J.; Claes, P.; De Clercq, E. *J. Med. Chem.* **1995**, *38*, 826−835.
(9) Verheggen, I.; Van Aerschot, A.; Toppet, S.; Snoeck, R.; Janssen, G.; Balzarini, J.; De Clercq, E.; Herdewijn, P. *J. Med. Chem.* **1993**, *36*, 2033−2040.
(10) Johnson, A. A.; Ray, A. S.; Hanes, J.; Suo, Z.; Colacino, J. M.; Anderson, K. S.; Johnson, K. A. *J. Biol. Chem.* **2001**, *276*, 40847−40857.
(11) Huttermann, J. *Radiat. Environ. Biophys.* **1991**, *30*, 71−79.
(12) Abdoul-Carime, H.; Huels, M. A.; Illenberger, E.; Sanche, L. *J. Am. Chem. Soc.* **2001**, *123*, 5354−5355.
(13) Li, X.; Sanche, L.; Sevilla, M. D. *J. Phys. Chem. A* **2002**, *106*, 11248−11253.
(14) Li, X.; Sevilla, M. D.; Sanche, L. *J. Am. Chem. Soc.* **2003**, *125*, 8916−8920.
(15) Morris, S. M. *Mutat. Res.* **1993**, *297*, 39−51.
(16) Ogino, H.; Fujii, M.; Suzuki, T.; Michishita, E.; Ayusawa, D. *DNA Res.* **2002**, *9*, 25−29.
(17) Liu, P.; Burdzy, A.; Sowers, L. C. *Chem. Res. Toxicol.* **2002**, *15*, 1001−1009.
(18) Lasken, R. S.; Goodman, M. F. *J. Biol. Chem.* **1984**, *259*, 11491−11495.
(19) Schmittgen, T. D.; Dannenberg, K. D.; Horikoshi, T.; Lenz, H. J.; Dannenberg, P. V. *J. Biol. Chem.* **1994**, *269*, 16269−16275.
(20) Yu, H.; Eritja, R.; Bloom, L. B.; Goodman, M. F. *J. Mol. Biol.* **1993**, *268*, 15935−15943.
(21) Henderson, J. P.; Byun, J.; Mueller, D. M.; Heincke, J. W. *Biochemistry* **2001**, *40*, 2052−2059.
(22) Henderson, J. P.; Byun, J.; Takeshita, J.; Heinecke, J. W. *J. Biol. Chem.* **2003**, *278*, 23522−23528.
(23) Singh, U. P.; Ghose, R.; Ghose, A. K.; Sodhi, A.; Singh, S. M.; Singh, R. K. *J. Inorg. Biochem.* **1989**, *37*, 325−339.
(24) Singh, S.; Singh, R.; Babbar, P.; Singh, U. P. *Transition Met. Chem. (London)* **2000**, *25*, 9−16.
(25) Stewart, R. F.; Jensen, L. H. *Acta Crystallogr.* **1967**, *23*, 1102−1105.
(26) Fallon, L., III. *Acta Crystallogr.* **1973**, *B29*, 2549.
(27) Sternglanz, H.; Bugg, C. E. *Biochim. Biophys. Acta* **1975**, *378*, 1−11.
(28) Sternglanz, H.; Freeman, G. R.; Bugg, C. E. *Acta Crystallogr.* **1975**, *B31*, 1393−1395.
(29) Nowak, M. J. *Nucleic Acid Bases Isolated in Gaseous Matrixes* (in Polish). Dissertation for D.Sc. Degree (Habilitation), Instytut Fizyki PAN, Warszawa, Poland, 1993.
(30) Szczepaniak, K.; Person, W. B.; Leszczynski, J.; Kwiatkowski, J. S. *Pol. J. Chem.* **1998**, *72*, 402−420.
(31) Graindourze, M.; Smets, J.; Zeegers-Huyskens, Th.; Maes, G. *J. Mol. Struct.* **1990**, *222*, 345−364.
(32) Barnes, A. J.; Stuckey, M. A.; Le Gall, L. *Spectrochim. Acta, Part A* **1984**, *40A*, 419−431.
(33) Szczesniak, M.; Nowak, M. J.; Rostkowska, H.; Szczepaniak, K.; Person, W. B.; Shugar, D. *J. Am. Chem. Soc.* **1983**, *105*, 5969−5976.
(34) Harsànyi, L.; Csàszàr, P.; Csàszàr, A.; Boggs, J. E. *Int. J. Quantum Chem.* **1986**, *24*, 799−815.
(35) Chin, S.; Scott, I.; Szczepaniak, K.; Person, W. B. *J. Am. Chem. Soc.* **1984**, *106*, 3415−3422.
(36) Ivanov, Yu.; Plokhotnichenko, A. M.; Radchenko, E. D.; Sheina, G. G.; Blagoi, Yu. P. *J. Mol. Struct.* **1995**, *372*, 91−100.
(37) Maltese, M.; Pesserini, S.; Nunziante-Cesaro, S.; Dobos, S.; Harsànyi, L. *J. Mol. Struct.* **1984**, *116*, 49−65.
(38) Graindourze, M.; Grootaers, T.; Smets, J.; Zeegers-Huyskens, Th.; Maes, G. *J. Mol. Struct.* **1990**, *237*, 389−410.
(39) Stepanian, S. G.; Radchenko, E. D.; Sheina, G. G.; Blagoi, Yu. P. *Biofizika* **1989**, *34*, 753−757.
(40) Florián, J.; Hrouda, V. *Spectrochim. Acta, Part A* **1993**, *49A*, 921−938.
(41) Smorygo, N. A.; Ivin, B. A. *Khim. Geterotsikl. Soedin.* **1975**, *1*, 105−113.
(42) Aamouche, A.; Ghomi, M.; Coulombeau, C.; Jobic, H.; Grajcar, L.; Baron, M. H.; Baumruk, V.; Turpin, P. Y.; Henriet, C.; Berthier, G. *J. Phys. Chem.* **1996**, *100*, 5224−5234.
(43) Susi, H.; Ard, J. S. *Spectrochim. Acta, Part A* **1971**, *27A*, 1549−1562.
(44) Allan, J. R.; McCloy, B. *Thermochim. Acta* **1992**, *208*, 133−137.
(45) Rastogi, V. K.; Mital, H. P.; Sharma, S. N. *Indian J. Phys., B* **1990**, *64B*, 312−316.
(46) Sanyal, N. K.; Srivastava, S. L.; Goel, R. K. *Indian J. Phys., B* **1977**, *52B*, 108−115.
(47) Singh, U. P.; Singh, B. N.; Ghose, A. K.; Singh, R. K.; Sodhi, A. *J. Inorg. Biochem.* **1991**, *44*, 277−282.
(48) Villa, J. F.; Nelson, H. C. *J. Indian Chem. Soc.* **1978**, *55*, 631−636.
(49) Rai, J. N. *Proc. Indian Acad. Sci., Chem. Sci.* **1990**, *102*, 687−691.
(50) Rai, J. N. *Indian J. Phys., B* **1983**, *57B*, 241−245.
(51) Zwierzchowska, Z.; Dobrosz-Teperek, K.; Lewandowski, W.; Kołos, R.; Bajdor, K.; Dobrowolski, J. Cz.; Mazurek, A. P. *J. Mol. Struct.* **1997**, *410−411*, 415−420.
(52) Dobrosz-Teperek, K.; Zwierzchowska, Z.; Lewandowski, W.; Bajdor, K.; Dobrowolski, J. Cz.; Mazurek, A. P. *J. Mol. Struct.* **1998**, *470*, 115−125.
(53) Bednarek, E.; Dobrowolski, J. Cz.; Dobrosz-Teperek, K.; Sitkowski, J.; Kozerski, L.; Lewandowski, W.; Mazurek, A. P. *J. Mol. Struct.* **2000**, *554*, 233−243.
(54) Witowska, J.; Dobrowolski, J. Cz.; Dobrosz-Teperek, K.; Lewandowski, W.; Mazurek, A. P. 14th International Mass Spectrometry Conference, Tempere, Finland, 1997.
(55) Bednarek, E.; Dobrowolski, J. Cz.; Dobrosz-Teperek, K.; Sitkowski, J.; Kozerski, L.; Lewandowski, W.; Mazurek, A. P. *J. Mol. Struct.* **1999**, *482−483*, 333−337.
(56) Dobrosz-Teperek, K.; Dobrowolski, J. Cz.; Kołos, R.; Lewandowski, W.; Mazurek, A. P. *J. Mol. Struct.* **2001**, *563−564*, 395−401.
(57) Frisch, M. J.; Trucks, G. W.; Schlegel, H. B.; Scuseria, G. E.; Robb, M. A.; Cheeseman, J. R.; Montgomery, J. A., Jr.; Vreven, T.; Kudin, K. N.; Burant, J. C.; Millam, J. M.; Iyengar, S. S.; Tomasi, J.; Barone, V.; Mennucci, B.; Cossi, M.; Scalmani, G.; Rega, N.; Petersson, G. A.; Nakatsuji, H.; Hada, M.; Ehara, M.; Toyota, K.; Fukuda, R.; Hasegawa, J.; Ishida, M.; Nakajima, T.; Honda, Y.; Kitao, O.; Nakai, H.; Klene, M.; Li, X.; Knox, J. E.; Hratchian, H. P.; Cross, J. B.; Adamo, C.; Jaramillo, J.; Gomperts, R.; Stratmann, R. E.; Yazyev, O.; Austin, A. J.; Cammi, R.; Pomelli, C.; Ochterski, J. W.; Ayala, P. Y.; Morokuma, K.; Voth, G. A.;

Salvador, P.; Dannenberg, J. J.; Zakrzewski, V. G.; Dapprich, S.; Daniels, A. D.; Strain, M. C.; Farkas, O.; Malick, D. K.; Rabuck, A. D.; Raghavachari, K.; Foresman, J. B.; Ortiz, J. V.; Cui, Q.; Baboul, A. G.; Clifford, S.; Cioslowski, J.; Stefanov, B. B.; Liu, G.; Liashenko, A.; Piskorz, P.; Komaromi, I.; Martin, R. L.; Fox, D. J.; Keith, T.; Al-Laham, M. A.; Peng, C. Y.; Nanayakkara, A.; Challacombe, M.; Gill, P. M. W.; Johnson, B.; Chen, W.; Wong, M. W.; Gonzalez, C.; Pople, J. A. *Gaussian 03*, Revision B.1; Gaussian, Inc.: Pittsburgh, PA, 2003.

(58) Barone, V.; Minichino, C. *THEOCHEM* **1995**, *330*, 365−376.

(59) Barone, V. *J. Chem. Phys.* **2004**, *120*, 3059−3065.

(60) Papamokos, G. V.; Demetropoulos, I. N. *J. Phys. Chem. A* **2004**, *108*, 7291−7300.

(61) Ozimiński, W. P.; Dobrowolski, J. Cz.; Mazurek, A. P. *THEOCHEM* **2004**, *680*, 107−115.

(62) Alcolea-Palafox, M. *Int. J. Quantum Chem.* **2000**, *77*, 661−684.

(63) Tsuzuki, S.; Lüthl, H. P. *J. Chem. Phys.* **2001**, *114*, 3949−3957.

(64) Jamróz, M. H. *Vibrational Energy Distribution Analysis VEDA 4.0*; Drug Institute: Warsaw, Poland, 2004.

(65) Alcolea-Palafox, M.; Rastogi, V. K. *Spectrochim. Acta, Part A* **2002**, *58*, 411−440.